medRxiv preprint doi: https://doi.org/10.1101/2024.05.16.24307410; this version posted May 16, 2024. The copyright holder for this preprint (which was not certified by peer review) is the author/funder, who has granted medRxiv a license to display the preprint in perpetuity. It is made available under a CC-BY 4.0 International license .

Using models to identify the causes of pre-symptomatic transmission from human infection data

Kayla Zhang[1], **Damie Pak**[1], **& Megan A. Greischar**[1]

[1]Department of Ecology and Evolutionary Biology, Cornell University, 215 Tower Rd, Ithaca, NY 14853, United States

Corresponding author: kz232@cornell.edu

Abstract. When disease transmission can precede symptom onset, containing outbreaks requires distinct strategies, like active surveillance. Yet it is rarely clear in advance when such interventions are needed, especially for emerging pathogens. Predicting pre-symptomatic transmission would be easier with knowledge of the within-host dynamics that enable pre-symptomatic transmission. To investigate those dynamics, we survey controlled human infection (CHI) trials with viral agents, which contain data on incubation times, infection duration, and transmission potential following inoculation with a known dose. We find that all studies report information on the duration of viral shedding, but few report the timing of symptoms. Only one study provided data on the timing of shedding and symptoms for individual participants, following norovirus inoculation. We apply a statistical model to individual time series to show significantly greater potential for pre-symptomatic transmission with faster viral replication, but no evidence for a tradeoff between transmission rate and duration during the pre-symptomatic phase. We then compare within-host models of pathogen replication, immune clearance, and symptom onset to identify plausible assumptions about the causes of pre-symptomatic transmission. We recover the pattern that peak shedding can precede symptom onset if we assume that symptoms are triggered by immune responses rather than pathogen abundance. Only by relaxing the standard assumption of exponential growth can we recover the pattern that faster viral replication enables pre-symptomatic transmission. Thus, data on symptom onset in CHI trials, paired with models, can illuminate the within-host dynamics underpinning pre-symptomatic transmission, guiding efforts to improve control strategies.

Significance statement. The COVID-19 pandemic was exacerbated by the potential for transmission before symptoms. Yet the causes of pre-symptomatic transmission remain unclear, hindering efforts to predict disease spread and tailor control efforts for novel pathogens. For known pathogens, the potential for pre-symptomatic transmission varies across individuals, but patterns may emerge from controlled human infection (CHI) trials. We surveyed CHI trials, finding that only one reported data on individual participants. We fit a simple model to those data, finding that faster viral replication correlates with pre-symptomatic transmission. We used more detailed models to identify plausible assumptions about the causes of symptom onset, e.g., that immune responses trigger symptoms. Thus, applying models to CHI trial data gives insight into the drivers of pre-symptomatic transmission.

NOTE: This preprint reports new research that has not been certified by peer review and should not be used to guide clinical practice.

medRxiv preprint doi: https://doi.org/10.1101/2024.05.16.24307410; this version posted May 16, 2024. The copyright holder for this preprint (which was not certified by peer review) is the author/funder, who has granted medRxiv a license to display the preprint in perpetuity. It is made available under a CC-BY 4.0 International license .

Keywords. controlled human infection trial, viral infection, transmission-duration tradeoff, within-host model, norovirus

The authors declare no competing interest.

Data availability. Full code to mine data and reproduce analyses and figures is available at github.com/greischarlab/transmission-modeling.

Acknowledgements. We thank Chadi Saad-Roy and Nicole Mideo for helpful discussion. This work was supported by the Cornell University College of Agricultural Sciences (M.A.G.), and the Cornell Institute of Host-Microbe Interactions & Disease Undergraduate Research Experience (K.Z.).

medRxiv preprint doi: https://doi.org/10.1101/2024.05.16.24307410; this version posted May 16, 2024. The copyright holder for this preprint (which was not certified by peer review) is the author/funder, who has granted medRxiv a license to display the preprint in perpetuity. It is made available under a CC-BY 4.0 International license .

1 Introduction

When diseases can be transmitted before symptom onset (pre-symptomatic transmission), controlling outbreaks is more difficult [1]. The COVID-19 pandemic exemplifies this challenge: a meta-analysis revealed that up to 69 percent of transmission was from pre-symptomatic hosts [2]. In contrast, SARS-CoV demonstrated far less pre-symptomatic transmission and was contained [1]. The variation in pre-symptomatic transmission, even among related pathogens, makes it difficult to anticipate how best to control emerging pathogens. Hence recent theory has focused on when and why pathogens evolve pre-symptomatic transmission [3–5]. Yet anticipating pre-symptomatic transmission remains difficult due to lack of clarity about the within-host dynamics that govern the relative timing of host infectiousness and symptoms.

Pathogens' potential to transmit is classically assumed to scale with their rate of replication within the host [6]. That assumption finds support in positive correlations between transmission potential and pathogen load observed in a range of systems [7], including HIV [8] and dengue [9]. Since symptoms are ultimately a consequences of pathogen replication, symptom onset might also be expected to occur earlier with faster replication rates. However, the relationship between pathogen load and symptoms is less clear, except in extreme cases such as HIV progressing to AIDS [8]. Symptoms could be directly correlated to pathogen load, for example, through toxins secreted by pathogens [10–12]. Faster within-host replication may be expected to hasten disease progression, including the onset of symptoms, as it does in HIV [8,13]. Alternatively, symptoms could be triggered by the immune response, as in the case of fever [14–16]. Faster pathogen replication could also hasten upregulation of immune defenses, potentially leading to more rapid clearance of faster replicating viral strains as shown in dengue [17]. Without a clear understanding of the links between symptom onset and transmission, it is impossible to anticipate constraints on pathogen evolution.

Distinct from the influence of replication rates, the initial dose could also influence symptom onset. A higher inoculum dose could increase the frequency of pre-symptomatic transmission by decreasing the time required for a pathogen to replicate to densities sufficient for the host to begin shedding appreciable amounts of infectious virions. Alternately, a higher inoculum dose could reduce pre-symptomatic transmission by triggering an immune response more quickly, leading to either the rapid onset of immune- or pathogen-mediated symptoms. Accordingly, one potential secondary purpose of masking is to limit the initial viral load to which an individual is exposed, which appears to lessen the severity of symptoms in respiratory diseases like SARS-CoV-2 [18–20], but the consequences for the timing of symptom onset are unclear. For some bacterial pathogens, such as *Chlamydophila caviae*, a higher inoculum dose is linked to greater upregulation of immune responses and pathology [21], while a lower inoculum dose may prevent activation of the host immune response across bacterial pathogens [22].

Data to investigate the role of pathogen traits and dose in promoting pre-symptomatic transmission are obtainable from controlled human infection (CHI) trials. In CHI trials, researchers are able to study acute infection dynamics by inoculating volunteers with a known dose of a pathogenic organism deemed sufficiently low-risk [23]. These studies are useful for acquiring precise data that cannot be obtained from observational studies of natural infections, including inoculum dose, and times of infection and symptom onset [24–27]. These

medRxiv preprint doi: https://doi.org/10.1101/2024.05.16.24307410; this version posted May 16, 2024. The copyright holder for this preprint (which was not certified by peer review) is the author/funder, who has granted medRxiv a license to display the preprint in perpetuity. It is made available under a CC-BY 4.0 International license .

data can illuminate the links between transmission and symptom onset.

To investigate the causes of pre-symptomatic transmission, we surveyed CHI trials of viral pathogens for data on the timing of symptom onset and transmission (that is, viral shedding). We subsequently focused on the only study showing both transmission timing and symptom onset for individual infections—a CHI trial with norovirus [28]—to identify how pre-symptomatic transmission varies with inoculum dose and viral replication rates. We fit a statistical model [29] to viral shedding data [28] to estimate replication rates and the time of peak shedding for individual infections. We classified infections as showing pre-symptomatic transmission when the estimated peak in pathogen shedding occurred prior to symptom onset and found no clear relationship with inoculum dose. We also found no evidence for a tradeoff between the rate and duration of pre-symptomatic transmission that is commonly assumed in theory [3–5]. Faster replication rates hastened peak shedding without changing symptom timing, enhancing pre-symptomatic transmission. By modifying a simple model of pathogen replication and clearance by immune effectors [30], we identified assumptions about viral replication and symptom onset consistent with empirical patterns. We found that peak shedding could only precede symptom onset when we assumed symptoms were triggered by increasing abundance of immune effectors, rather than pathogen load. We recovered a positive relationship between viral replication rate and pre-symptomatic transmission when we relaxed the assumption of exponential growth and incorporated a pathogen carrying capacity. Thus, individual data on pathogen shedding and symptom onset enable selection of plausible models for pre-symptomatic transmission.

2 Results

We first completed a meta-analysis of CHI trials to survey what data were reported regarding the timing of symptoms and transmission. We then used a statistical model [29] to estimate the timing of peak viral shedding as well as pathogen replication rates to determine trends in pre-symptomatic transmission among patients in a norovirus study [28]—the only study we found to include both viral load and symptom data at the individual level. Lastly, we modified a dynamical model [30] to identify assumptions that could give rise to empirical patterns.

2.1 Most CHI trials do not report relative timing of symptom onset and transmission

We found 31 CHI studies tracking viral shedding and/or symptom onset and duration (Fig. 1). CHI studies are summarized in Fig. 1, including (in order from left to right, top to bottom) SARS-CoV-2 [31], respiratory syncytial virus (RSV) [26, 32, 33], rhinovirus [27, 34–36], norovirus [25, 28, 37, 38], influenza B [39, 40], and influenza A [26, 40–56].

Most of these studies (16 of 31) presented these data as graphs, rather than reporting values in the text. Only 10 studies reported the requisite data needed to assess trends in pre-symptomatic transmission (shedding onset, shedding duration, and symptom onset), and only one study [28] reported these data for individual hosts. While a rhinovirus study

medRxiv preprint doi: https://doi.org/10.1101/2024.05.16.24307410; this version posted May 16, 2024. The copyright holder for this preprint (which was not certified by peer review) is the author/funder, who has granted medRxiv a license to display the preprint in perpetuity. It is made available under a CC-BY 4.0 International license .

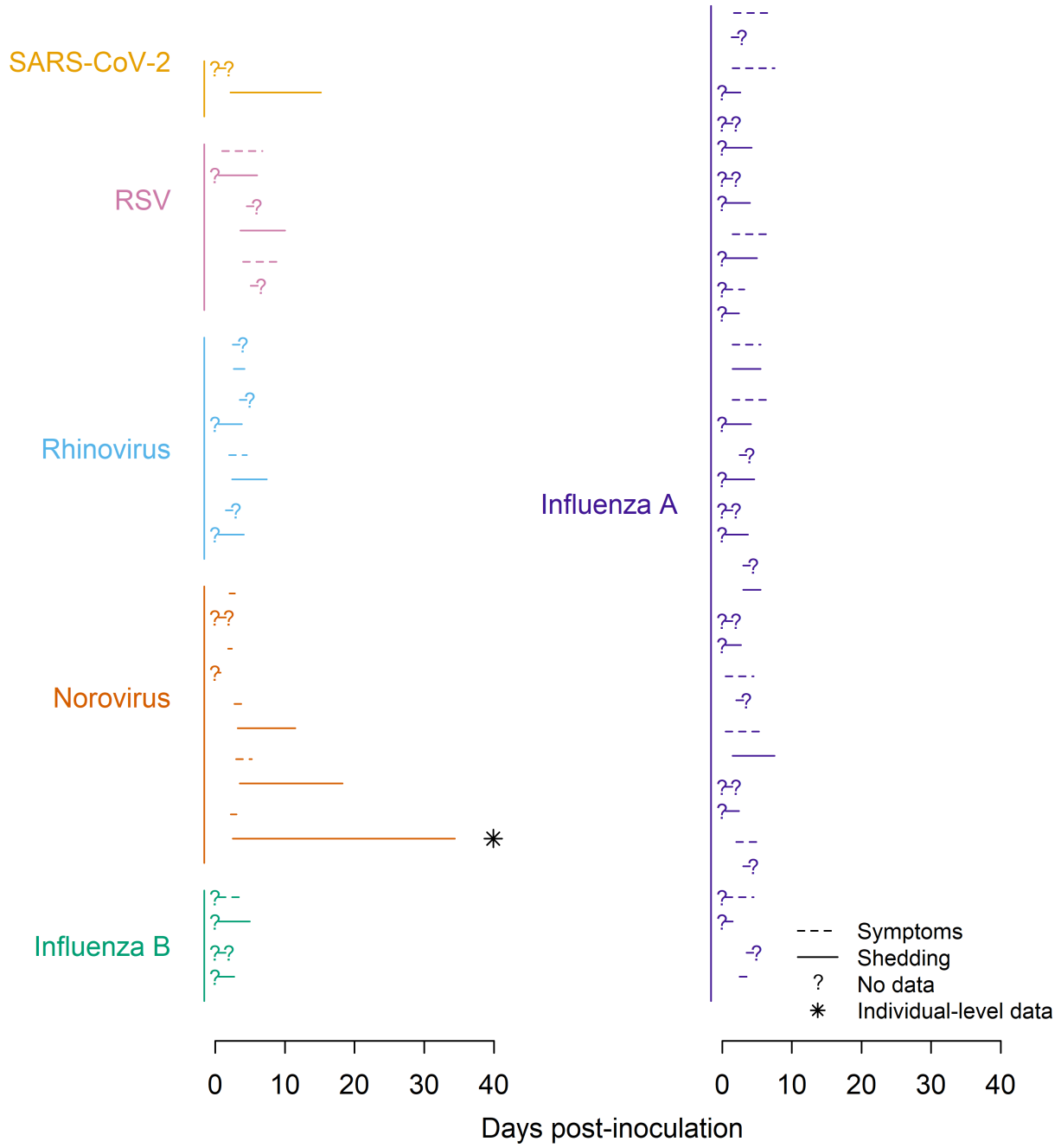

Figure 1: Most CHI studies do not report individual-level data on pathogen shedding and the timing of symptoms. Dotted lines indicate reported symptom onset and duration, while solid lines indicate shedding times. Question marks indicate unreported data on the onset and/or duration of shedding or symptoms. When the timing of onset was missing, we place the question mark at day 0. An asterisk indicates the only study that reports individual-level data for both shedding and symptom onset [28].

reported individual-level shedding data, symptoms were reported as averages across patients

medRxiv preprint doi: https://doi.org/10.1101/2024.05.16.24307410; this version posted May 16, 2024. The copyright holder for this preprint (which was not certified by peer review) is the author/funder, who has granted medRxiv a license to display the preprint in perpetuity. It is made available under a CC-BY 4.0 International license .

over time [34].

2.2 Faster viral replication associated with pre-symptomatic transmission

We used the viral shedding data reported by [28] to reconstruct the within-host trajectory, by fitting the rates of exponential growth and decline, and the timing and height of peak viral load. Peak viral shedding is likely to follow peak viral load in the gut by a number of hours, and gut transit times may vary substantially across individuals (reviewed in [57]). For simplicity, we assumed no variation in gut transit times within an individual over the time scale of the CHI trial, i.e., that the dynamics of viral shedding reflect the dynamics of viral abundance within the host. We later discuss how a lag between viral load and shedding could impact our results and conclusions. To estimate the trajectory of viral load, we fit a statistical model [29] to individual viral shedding data. The $\log_{10}$ viral load, $V(t)$, is defined as

$$V(t) = \frac{2P_1}{e^{-P_2(t-P_3)} + e^{P_4(t-P_3)}}, \tag{1}$$

where P_1 refers to the $\log_{10}$ peak viral load; P_2 and P_4 refer to the exponential growth and decay rates, respectively, of viral load; and P_3 refers to the time of peak viral load. Fitting a dynamical model would have required fitting many more parameters and making assumptions about initial conditions. The statistical model described in Eq. 1 required no assumptions about initial conditions and could be fit with the limited data available for each participant.

We defined pre-symptomatic transmission as occurring when peak viral shedding preceded symptom onset, on the logic that individuals shedding at their maximal rates prior to symptoms were likely to be infectious. When fit to data from [28], estimated individual trajectories show variation in the relative timing of peak shedding and symptom onset (Fig. 2, data and fitted trajectories for other patients in Fig. S1). The timing of peak shedding was not clear for two participants who were excluded from this analysis (Fig. S3). For other patients, viral shedding increased initially, then decreased, with the estimated time of peak shedding (P_3 in Eq. 1) either preceding or following symptom onset. For example, of the three individual infections shown in Fig. 2, only the first (A) exhibits pre-symptomatic transmission.

Across all infections with a clear peak in shedding, four out of fourteen participants exhibited pre-symptomatic transmission: three from the highest inoculum dose (4800 RT-PCR units) and one from the lowest inoculum dose (4.8 RT-PCR units) (Fig. 3A). We found a nonsignificant trend towards longer time delays between peak shedding and symptom onset at higher inoculation doses (Fig. 3A) and a significant negative correlation between estimated viral replication rate (P_2 parameter in Equation 1) and the delay between symptom onset and peak viral shedding (Fig. 3B, $p = 0.0182, \beta = -0.7436, R^2 = 0.3835, F = 7.465$). Thus, at high viral replication rates, pre-symptomatic transmission is more likely, sincehigher replication rates lead to significantly earlier peak shedding ($p = 0.0029$) while having no marked impact on symptom onset (Fig. S5). No other significant relationships between parameter values were found, though there was a nonsignificant correlation between rates of

medRxiv preprint doi: https://doi.org/10.1101/2024.05.16.24307410; this version posted May 16, 2024. The copyright holder for this preprint (which was not certified by peer review) is the author/funder, who has granted medRxiv a license to display the preprint in perpetuity. It is made available under a CC-BY 4.0 International license .

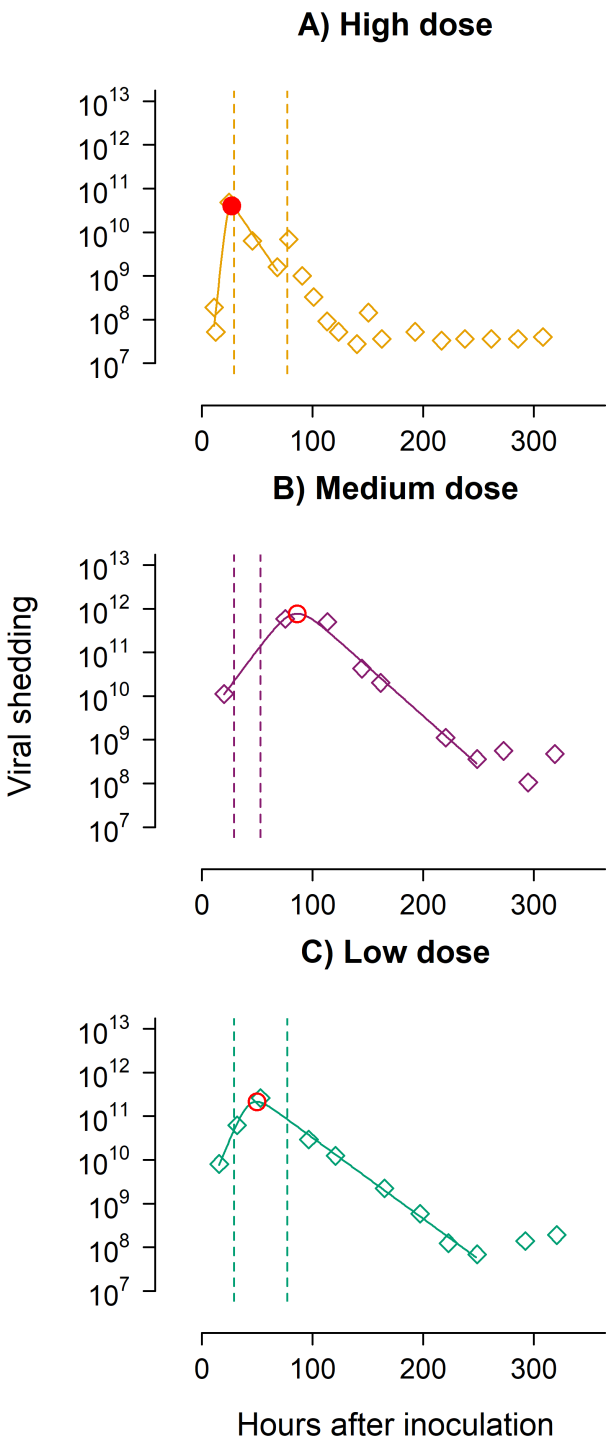

Figure 2: The relative timing of symptoms and shedding varies across participants. Panels A, B, and C show viral shedding over time for three participants (703, 722, and 724) infected with norovirus with varying inoculum doses (4.8, 48, and 4800 RT-PCR units, yellow, purple and green, respectively) from [28]. Open diamonds indicate observed viral shedding in the hours after inoculation with a solid line to indicate the best fit parameterization of Eq. 1 to the data. The dotted vertical lines show the start and end of symptoms. A red circle shows estimated peak viral shedding; a closed red circle indicates peak shedding preceded symptoms (pre-symptomatic transmission, A only), open red circles show peak shedding following symptom onset (post-symptomatic transmission, B and C).

exponential expansion (replication rates) and decay. We also calculated the average shedding prior to symptom onset for each participant demonstrating a clear peak to serve as a proxy for transmission rate and used linear regression to test for a correlation with the time until symptom onset. Theory often assumes a tradeoff between the duration and rate of transmission prior to symptoms (e.g., [3]), but we found no correlation between transmission rate prior to symptoms and the time until symptom onset (Fig. 3C).

medRxiv preprint doi: https://doi.org/10.1101/2024.05.16.24307410; this version posted May 16, 2024. The copyright holder for this preprint (which was not certified by peer review) is the author/funder, who has granted medRxiv a license to display the preprint in perpetuity. It is made available under a CC-BY 4.0 International license .

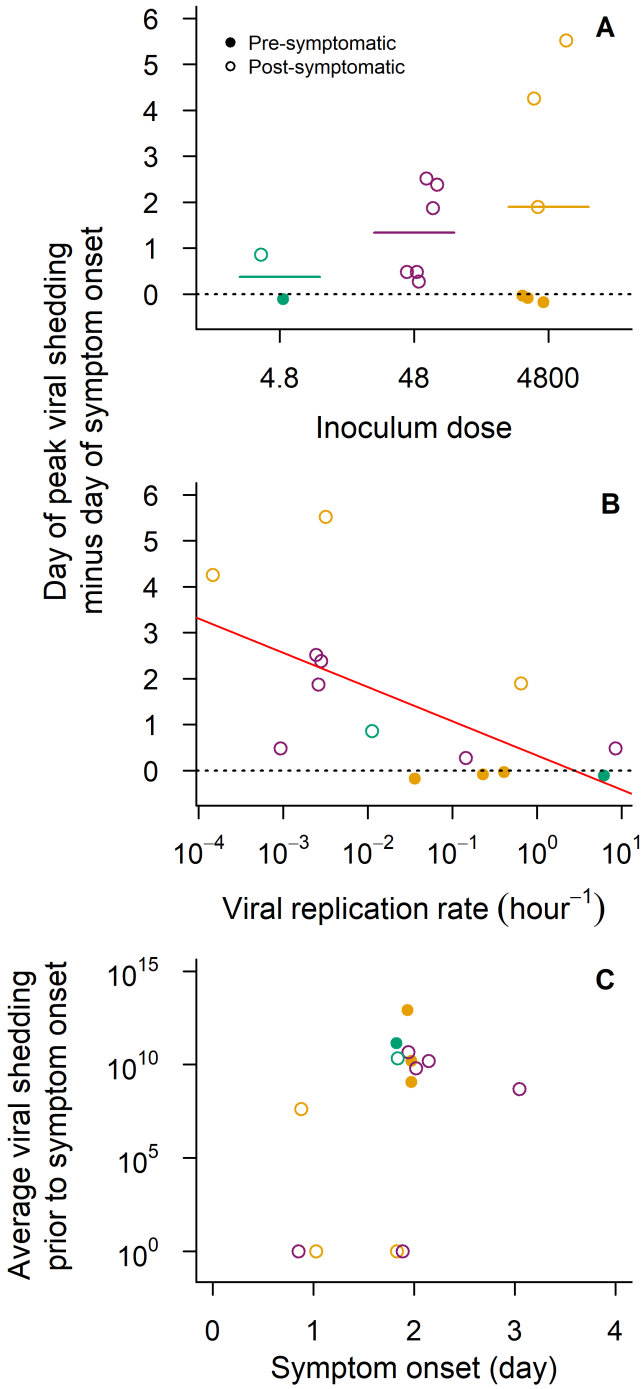

Figure 3: Individual level norovirus data [28] yield insight into the causes and consequences of pre-symptomatic transmission. (A) There is no significant dose-dependence in the relative timing of symptoms and shedding. Low, medium and high doses (4.8, 48 and 4800) indicated by green, purple and orange, with horizontal bars to indicate the average delay for each dose. (B) Pre-symptomatic transmission is more common in infections with faster replication rates (P_2, Eq. 1). As viral replication rate increases, it is more likely that the peak of viral shedding will precede symptom onset ($p = 0.0182, \beta = -0.7436, R^2 = 0.3835, F = 7.465$). (C) There is no clear relationship between average transmission rate prior to symptoms and the time until symptom onset.

Our definition of pre-symptomatic transmission is conservative and likely to underestimate pre-symptomatic transmission, since an individual could be infectious before peak viral shedding. The inoculum doses used (4.8, 48, and 4800 genomic copies/mL liquid feces) were vastly lower than the number of genome copies/g feces detected later on (as apparent in Fig. S1). If we instead defined pre-symptomatic transmission less conservatively as shedding preceding symptom onset, the proportion of participants experiencing experiencing

medRxiv preprint doi: https://doi.org/10.1101/2024.05.16.24307410; this version posted May 16, 2024. The copyright holder for this preprint (which was not certified by peer review) is the author/funder, who has granted medRxiv a license to display the preprint in perpetuity. It is made available under a CC-BY 4.0 International license .

pre-symptomatic transmission increases slightly (5 out of 16, Fig. S4). Because this measure does not reference participants' viral shedding trajectories, we included the two participants whose infections had unclear timing of peak shedding in this analysis. Using that less conservative definition, no participants from the low dose group exhibit pre-symptomatic transmission and there is a slight trend towards more pre-symptomatic transmission from the medium and high dose groups (Fig. S4A). However, even with this less conservative definition, we still find that pre-symptomatic transmission is significantly more likely with increasing viral replication rates (Fig. S4B, $p = 0.0064$).

2.3 Immune threshold for symptoms and pathogen carrying capacity can reproduce empirical patterns

The results of our analyses of the data from [28] motivate the second part of this study, to identify a within-host model consistent with the two main patterns identified from the data reported by [28]: (1) that peak shedding can precede symptom onset (pre-symptomatic transmission); and (2) that faster viral replication rates extend the duration of pre-symptomatic transmission. We extend a simple model of exponential viral replication and immune clearance [30] to incorporate symptom onset and determine the plausibility of symptoms arising due to either a pathogen load threshold (s_P), or an immune effector threshold (s_X). Assuming a pathogen load threshold, we find that peak viral load can never precede symptom onset. If peak viral load falls below the symptom threshold s_P, then the simulated infection will never cause symptoms (Fig. 4A, left). Alternately, if the symptom threshold s_P is less than peak viral load, then viral load must cross the threshold before it peaks (Fig. 4A, right). Because peak viral load can never precede symptom onset, pre-symptomatic transmission as seen in the data is not possible, only post-symptomatic and asymptomatic transmission.

When the symptom threshold is determined by immune effector abundance, both pre-symptomatic and post-symptomatic transmission are possible (i.e., peak pathogen abundance can precede or follow symptom onset, Fig. 4B). Our analysis shows that as the replication rate r increases, the simulated outcome will switch from pre- to post-symptomatic, a pattern we confirm with simulations (Fig. S7A, see Methods for details). Thus, this model fails to recover the empirical pattern that faster replication extends the time window for pre-symptomatic transmission (Fig. 3B).

Finally, we investigate the impact of incorporating a pathogen carrying capacity on pre-symptomatic transmission. Implementing a carrying capacity would not broaden the range of dynamics possible from a pathogen-based symptom threshold, since there would still be no way for pathogen load to peak and then pass the symptom threshold. Retaining the assumption of symptom onset based on an immune effector abundance threshold, we impose a pathogen carrying capacity, implying that pathogen replication is resource-limited. We again find that peak pathogen abundance can precede or follow symptom onset (both pre- and post-symptomatic transmission, Fig. 4C). By relaxing the assumption of exponential pathogen growth, we recover the empirical pattern that as replication rate increases, there is a longer period of time between peak pathogen load and symptom onset (pre-symptomatic transmission, Fig. S7B, *cf.* Fig. 3B).

medRxiv preprint doi: https://doi.org/10.1101/2024.05.16.24307410; this version posted May 16, 2024. The copyright holder for this preprint (which was not certified by peer review) is the author/funder, who has granted medRxiv a license to display the preprint in perpetuity. It is made available under a CC-BY 4.0 International license .

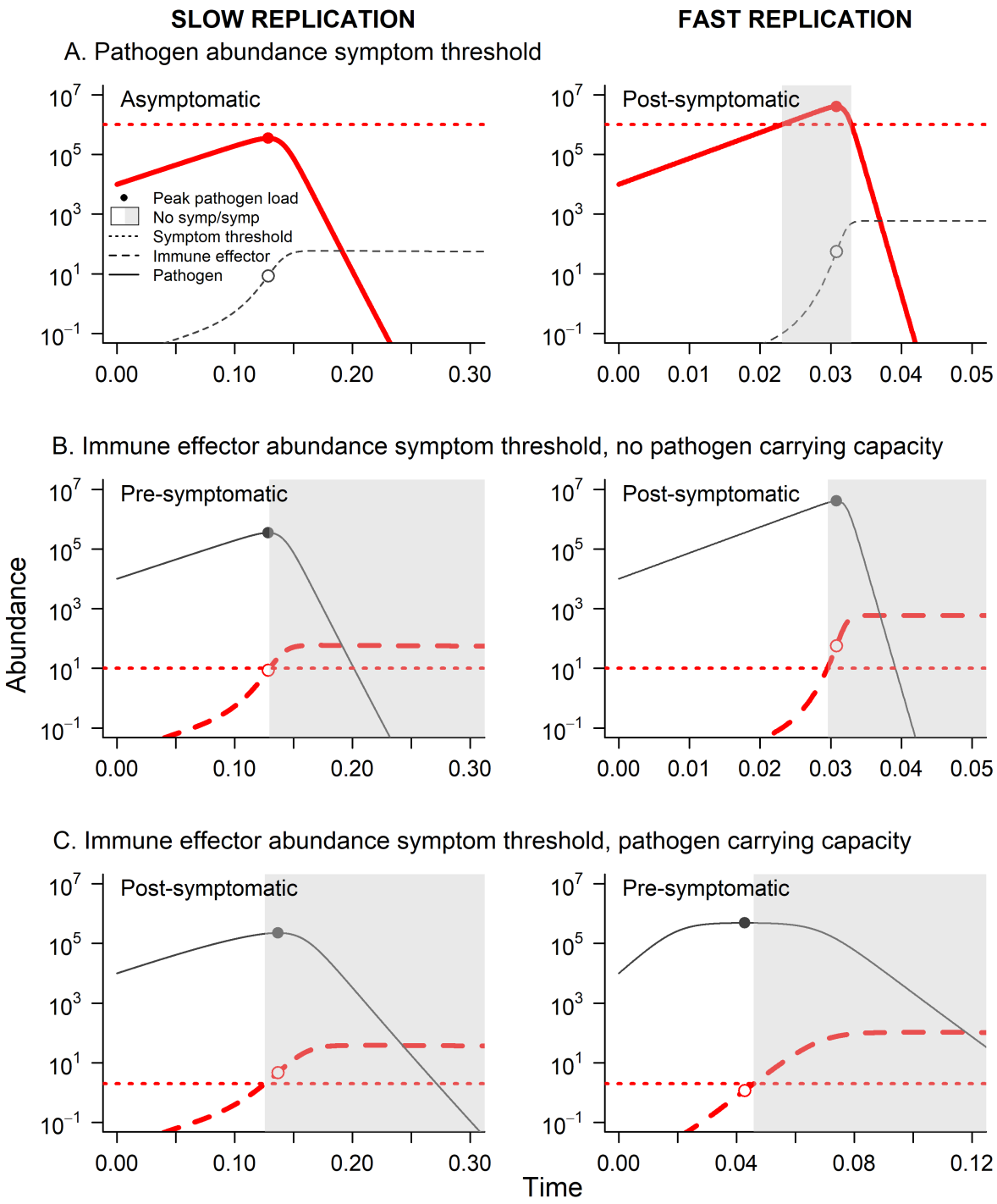

Figure 4: Models reveal plausible (and implausible) drivers of pre-symptomatic transmission. Bolded red lines indicate the quantity that triggers symptoms when its abundance exceeds the threshold. Peak pathogen load occurs when the abundance of immune effectors $X = r/k$ (indicated by an open point, with a closed point to show the corresponding pathogen abundance, see main text for details). *Caption continues.*

medRxiv preprint doi: https://doi.org/10.1101/2024.05.16.24307410; this version posted May 16, 2024. The copyright holder for this preprint (which was not certified by peer review) is the author/funder, who has granted medRxiv a license to display the preprint in perpetuity. It is made available under a CC-BY 4.0 International license .

Figure 4: *Caption continued.* (A) With a pathogen abundance symptom threshold ($s_P = 10^6$), the model can only produce asymptomatic or post-symptomatic transmission (when replication is slow or fast, respectively). (B) With an immune effector-abundance symptom threshold ($s_X = 10$), the model can produce post- and pre-symptomatic transmission, with fast and slow replication (respectively). (C) Retaining an immune effector abundance symptom threshold ($s_X = 2$) and relaxing the assumption of exponential pathogen growth, pre-symptomatic transmission is more likely with faster replication. In all panels, $k = 3.5$, $\alpha = 1$, $d = 0.5$, and $\gamma = 10^{-4}$. Replication rates were $r = 30$ (left panels) or $r = 200$ (right panels). In panel C, the carrying capacity was defined as $\theta = 5 \times 10^5$.

3 Discussion

Pre-symptomatic transmission plays an important role in propagating outbreaks of diseases, including SARS-CoV-2 [58–60]. Better understanding of how within-host dynamics determine the relative timing of transmission and symptoms would improve prevention strategies by enabling predictions about the host and pathogen characteristics likely to promote pre-symptomatic transmission. We show that achieving that level of understanding could be greatly facilitated by applying within-host models to the invaluable data generated by CHI trials. We find that individual time series are rarely reported from viral CHI trials, but when reported (as in [28]), those individual-level data on the timing of transmission and symptoms can be leveraged to pare down the plausible causes and potential consequences of pre-symptomatic transmission. By analyzing previously reported data [28], we uncovered a positive relationship between pathogen replication rate and pre-symptomatic transmission. We found no evidence for dose-dependence or for a tradeoff between transmission rate and duration during pre-symptomatic infection. Subsequent analysis revealed that the model most consistent with the data was one in which symptom onset is triggered by immune effector abundance exceeding a threshold and in which pathogen populations are regulated by both resource limitation and immune clearance. Our study provides proof-of-concept for how within-host models can be used to extend the inferences that can be drawn from CHI trials.

We found that pathogen replication rate is positively associated with pre-symptomatic transmission, whether our measure was conservative (peak shedding prior to symptom onset) or not (shedding onset prior to symptom onset). Such a pattern may also play out across pathogen species, with faster-replicating pathogens exhibiting earlier peak viral loads and pre-symptomatic transmission. SARS-CoV-2 and H1N1pdm09, responsible for the 2009 influenza pandemic, display early peak viral loads and appreciable amounts of pre-symptomatic transmission, while SARS-CoV and MERS-CoV exhibit later peak viral loads and little pre-symptomatic transmission [61]. Individual-level data from CHI trials could reveal whether this pattern holds across diverse pathogens and whether there is any phylogenetic signal of pre-symptomatic transmission. Although not a given, if pre-symptomatic transmission is a trait likely to be held in common across closely relatives, it would enhance capacity to predict spread of emerging pathogens. Distinct from the possibility of phylogenetic patterns, predictive ability would also be improved by identifying tradeoffs that constrain the evolution

medRxiv preprint doi: https://doi.org/10.1101/2024.05.16.24307410; this version posted May 16, 2024. The copyright holder for this preprint (which was not certified by peer review) is the author/funder, who has granted medRxiv a license to display the preprint in perpetuity. It is made available under a CC-BY 4.0 International license .

of pre-symptomatic transmission.

Our analysis suggests a notable absence of evidence for tradeoffs. Faster replication promotes pre-symptomatic transmission by hastening peak pathogen shedding, but has no impact on the timing of symptom onset (Fig. S5). One difficulty is that symptom onset was recorded in whole days, while fitted estimates of peak shedding achieve higher resolution. Yet even if we do not rely on fitted estimates and instead consider the days elapsing between onset of symptoms and shedding, we still find that pre-symptomatic shedding is more likely with faster replicating virus (Fig. S4B). Moreover, there is no relationship between transmission rate (i.e., average shedding) prior to symptoms and the time until symptom onset, which belies the expected tradeoff between transmission and duration for the initial latent (pre-symptomatic) phase of infection, commonly assumed in theory [3–5, 62]. While such a transmission-duration tradeoff is highly relevant for some viruses (e.g., HIV, [8, 13]), other constraints may be needed to explain the lack of evolution towards ever faster replication in less deadly viral infections [63]. Our within-host modeling suggests that resource limitation may be an important constraint, and one that has received more attention in recent models of within-host viral dynamics (e.g., [17]). Theory suggests that resource limitation can generate a tradeoff between transmission early versus late in infection (e.g., in malaria parasites, [64, 65]). If resource limitation imposes a tradeoff between pre- and post-symptomatic transmission, then latency could evolve over the course of an epidemic, with traits that enhance infectiousness later in infection favored as transmission becomes more difficult [66].

One area that warrants further attention is the role of replication rates in modulating the time required for virus to exit the host. In the case of respiratory viruses, the delay between viral replication and transmission would likely be short, given the brief time required for a viral particle to travel from the respiratory tract to the nose or mouth to then exit the host via activities such as breathing, coughing, and sneezing. The delay is likely greater for pathogens colonizing the lower respiratory tract, where the site of aerosol formation is farther from the nose or mouth [67]. In the case of enteric pathogens, the lag between replication and fecal shedding is determined by the gut transit time. For simplicity, we assumed no such time lag, but incorporating gut transit times would not alter our finding that pathogen-based symptom thresholds are inconsistent with the data. Whatever the gut transit time, peak pathogen pathogen load should always precede peak shedding. If symptoms are assumed to occur when pathogen load crosses a threshold, then shedding must necessarily follow symptoms, and hence that assumption cannot recapitulate the empirical pattern that peak shedding can precede symptom onset (Fig. 3). This result adds to findings in other systems that a within-host abundance threshold is insufficient to explain symptom onset (e.g., the 'pyrogenic threshold' of malaria parasite numbers required to trigger malaria fevers, [68]). The implications of other assumptions about symptom onset will depend on how viral replication rates influence gut transit times. If a higher replication rate results in shorter gut transit time, that could hasten both shedding and the onset of symptoms like diarrhea, making the impact on pre-symptomatic transmission difficult to predict. Gut transit times are known to vary person-to-person by a factor of days, as well as within individuals day-to-day [57]. For enteric pathogens, understanding how gut transit times change following infection, including variability across individual hosts, would enhance efforts to reconstruct within-host dynamics from CHI data.

Host immunity is also likely to influence pre-symptomatic transmission. Our simple model

medRxiv preprint doi: https://doi.org/10.1101/2024.05.16.24307410; this version posted May 16, 2024. The copyright holder for this preprint (which was not certified by peer review) is the author/funder, who has granted medRxiv a license to display the preprint in perpetuity. It is made available under a CC-BY 4.0 International license .

allows predictions for how multiple immune parameters—immune effector recruitment and loss rates, and pathogen kill rate per immune effector—impact pre-symptomatic transmission, enabling comparison with CHI shedding and symptom data [28]. More complex models could predict how specific kinds of immune effectors modulate viral replication, shedding, and symptoms; data on levels of immune effectors such as cytokines and antibodies are obtainable from CHI trials [31, 41, 42]. Coupling these data with model predictions could address a range of open questions, including whether vaccination alters the relative timing of symptom onset and transmission in individuals experiencing breakthrough infections, whether immuno-compromised patients are more or less likely to transmit pre-symptomatically, and the extent to which different types of immune effectors promote pre-symptomatic transmission. Further investigation into the impact of viral and host traits on pre-symptomatic transmission would aid public health efforts in predicting what pathogenic agents and host populations (for example, those with immunological memory through previous exposure or vaccinations versus those without) are more likely to transmit pre-symptomatically. It may then be possible to target interventions like testing, masking, or vaccination programs, where they will be most useful.

We found no consistent effect of inoculum dose, since the direction of the (nonsignificant) trend depended on how we defined pre-symptomatic transmission. The lack of a clear pattern makes sense given the potentially complex consequences of dose on disease progression and transmission. For the influenza virus, higher inoculum dose increases expression of inflammatory cytokines and recruitment of innate immune effectors [69]. Innate immune effectors may slow pathogen replication, but a greater inflammatory response could hasten symptom onset, so the net impact on pre-symptomatic transmission is challenging to predict. Similarly, in infections of *Vibrio cholerae*, higher dose allows for greater cooperative effects among bacteria enabling more efficient colonization of the gastrointestinal tract [70], which promotes both pathogen load and disease progression and makes it challenging to anticipate the impact on pre-symptomatic transmission. Yet for some pathogens, severe disease seems to require a minimum inoculum dose, including SARS-CoV-2 [71], MERS-CoV [72], and hepatitis C [73], suggesting that higher doses could hasten symptoms and thereby reduce pre-symptomatic transmission. The consequences of inoculum dose for pre-symptomatic transmission may be complex and nonlinear, but general patterns may still emerge. For example, slowed multiplication rates when population sizes are low (known as Allee effects) are thought to apply broadly across diverse organisms [74]. Models can provide insight into when and how limited inoculum doses slow initial replication of pathogenic organisms (e.g., fitting models to data from experimental rodent malaria infections, [75]). Applying models to CHI trial data would reveal whether relationships between dose and pre-symptomatic transmission are idiosyncratic or predictable across different pathogens.

We compared the dynamics of pre-symptomatic transmission for models assuming that symptoms result from crossing a threshold determined by pathogen load or immune effector abundance, but symptom onset could have multiple, related causes. Immune responses have been demonstrated to facilitate pathology in diseases such as COVID-19, influenza, and tuberculosis [76–78]. In COVID-19, symptoms vary considerably and the causes are multi-faceted: ranging from headache and sore throat to myalgia, chest pain, and abdominal pain for patients with severe infections [79]. Although sore throat is likely a result of immune activity and abdominal pain a result of cell death due to pathogen activity, the

medRxiv preprint doi: https://doi.org/10.1101/2024.05.16.24307410; this version posted May 16, 2024. The copyright holder for this preprint (which was not certified by peer review) is the author/funder, who has granted medRxiv a license to display the preprint in perpetuity. It is made available under a CC-BY 4.0 International license .

hypothesized causes of headache, myalgia, and chest pain remain conflicting and inconclusive [79]. Evidence suggests that loss of smell, one of the most characteristic symptoms of COVID-19, is likely caused by infection of cells associated with the olfactory sensory neurons by SARS-CoV-2. However, mucosal swelling and airflow obstruction, a result of immune activity, could also contribute to the phenomenon [80]. To account for a variety of causes, more complex models of symptom onset are needed to differentiate the impacts on pre-symptomatic transmission. Understanding the within-host dynamics that give rise to symptoms would help assess the generality of commonly assumed tradeoffs between transmission and duration, which has been increasingly questioned [63]. Individual-level data on the timing of symptoms and transmission could hasten advances in this key area.

Understanding the within-host causes of pre-symptomatic transmission is a prerequisite for predicting the epidemiological impact. For a given pathogenic organism, variation across individual hosts can have an outsize impact on the potential for outbreaks, with undiagnosed or misdiagnosed infections implicated in more superspreading events than unusually high contact rates [81]. Our analysis of individual infections reported by [28] suggests that—even controlling for viral genetic background and dose—there are considerable differences in both the propensity for pre-symptomatic transmission and replication rates, the latter of which varies across orders of magnitude (Fig. 3, S4). Individual-level data on the timing of symptoms, coupled with models of symptom onset, can reveal the mechanistic causes of pre-symptomatic transmission and offer insight into the intervention measures best-suited to containing outbreaks.

4 Methods

4.1 Survey of CHI trials for the transmission dynamics of viral pathogens

We searched for viral CHI studies on Google Scholar using the terms: "experimental OR controlled infection viral load shedding duration human." We then looked through the references of studies found during our search and included any pertinent additional trials. The last search performed was on November 5, 2023. Studies were included if the virus could be classified as enteric or respiratory, as the diseases they cause have symptoms that are easier to recognize.

We recorded mean or median onset and duration—whichever was available—for symptoms and shedding from the main text or tables directly when possible. If individual data were reported, we calculated the average duration and onset of shedding and transmission. Some studies reported symptom onset and duration as a participant-reported symptom score over time. We then estimated the onset and duration of shedding from the first and last reported timepoint with the mean/median symptom score greater than or equal to the minimum possible for a symptomatic individual. Some studies included multiple cohorts; for these we applied the above methods to data from only one cohort. For studies that investigated more than one disease, we separated datasets by virus [25, 26, 40].

medRxiv preprint doi: https://doi.org/10.1101/2024.05.16.24307410; this version posted May 16, 2024. The copyright holder for this preprint (which was not certified by peer review) is the author/funder, who has granted medRxiv a license to display the preprint in perpetuity. It is made available under a CC-BY 4.0 International license .

4.2 Identifying correlates of pre-symptomatic transmission

Atmar et al. [28] present shedding for 16 participants as plots, along with a table reporting the timing of symptoms. We digitized individual-level shedding data reported in plots using the **R** package 'metaDigitize' [82]. While data on symptoms were captured daily, data on viral shedding ranged from being captured multiple times a day to once every couple of days, depending on the availability of fecal samples. To fit the four parameters for Eq. 1, we minimized the sum squared error between observed $\log_{10}$ viral shedding and predicted $\log_{10}$ viral load using the `optim` function in **R 4.2.1**.

Eq. 1 describes acute infection [29], where pathogen populations grow and decline at constant rates. Some infections showed a low level of shedding for an extended period after a log-linear decline, a situation for which Eq. 1 was not designed. We therefore defined the end of acute infection—that is, the end of the time series we used to fit the model—as the first local minimum in viral shedding. We found similar qualitative results if we instead defined the end of acute infection as the first viral shedding value equal to or less than the abundance in the first fecal sample (*cf.* Figs. S1 and S2).

4.3 Defining a plausible within-host model for pre-symptomatic transmission

We modified the within-host model described in [30] by incorporating thresholds for symptom onset and allowing for a pathogen carrying capacity, θ. The model tracks the abundance of pathogen (P) and host immune effectors (X):

$$\frac{\mathrm{d}P}{\mathrm{d}t} = r\eta P - kXP, \tag{2}$$

$$\frac{\mathrm{d}X}{\mathrm{d}t} = \alpha - dX + \gamma kXP, \tag{3}$$

$$\text{where } \eta = \begin{cases} 1 & \text{(exponential growth)} \\ 1 - \frac{P}{\theta} & \text{(carrying capacity).} \end{cases}$$

As pathogen load increases, more immune cells are activated and more pathogens are killed upon contact. Unless otherwise indicated, the model assumes the pathogen population grows exponentially ($\eta = 1$), and it is only the host immunity that controls the pathogen population. Thus, even though pathogen load initially increases exponentially at rate r, it eventually declines due to the accompanying increase in immune effector abundance. The other parameters are the basal immune cell birth rate (α), the immune cell death rate (d), the immune cell recruitment rate (γ), and the immune cell kill rate of the pathogen (k), with values given in Table 1. We subsequently implement a carrying capacity for pathogen load ($\eta = 1 - P/\theta$, and $\theta = 5 \times 10^5$).

We assume symptoms (S) occurs when 1) pathogen load (P) crosses a threshold (s_P); or 2) when immune effector abundance (X) crosses a threshold (s_X).

Case 1:

$$S = \begin{cases} Present & \text{if } P \geq s_P \\ Absent & \text{else} \end{cases} \tag{4}$$

medRxiv preprint doi: https://doi.org/10.1101/2024.05.16.24307410; this version posted May 16, 2024. The copyright holder for this preprint (which was not certified by peer review) is the author/funder, who has granted medRxiv a license to display the preprint in perpetuity. It is made available under a CC-BY 4.0 International license .

Case 2:

$$S = \begin{cases} Present & \text{if } X \geq s_X \\ Absent & \text{else} \end{cases} \tag{5}$$

We varied viral replication rates (r) to examine their impact on the delay between symptom onset and peak pathogen load (time of peak pathogen load minus time of symptom onset). For simplicity, we assume that viral shedding is equal to viral load within the host with no time delay (e.g., a time delay associated with gut transit time for norovirus infections).

4.3.1 Analysis of immune effector symptom threshold with exponential viral replication

We analyze Eq. 2 and 3 to examine the relationship between peak pathogen load and the time of symptom onset under exponential growth ($\eta = 1$). By setting $dP/dt = 0$, we determine the time of peak pathogen load and solve for the corresponding immune effector abundance ($X = r/k$). Peak immune effector abundance follows peak pathogen abundance for the parameter values used here (Fig. S6), meaning that immune effector abundance is always increasing at peak pathogen load. Therefore, the key question is whether immune effector abundance at peak pathogen load (r/k) is above or below the symptom threshold (neglecting the case where peak immune effector abundance is equal to the symptom threshold). If above ($r/k > s_X$), then symptoms have already begun by the time pathogen abundance reaches its peak (post-symptomatic transmission). If below ($r/k < s_X$), then peak pathogen abundance (and hence shedding) will precede symptom onset (pre-symptomatic transmission).

medRxiv preprint doi: https://doi.org/10.1101/2024.05.16.24307410; this version posted May 16, 2024. The copyright holder for this preprint (which was not certified by peer review) is the author/funder, who has granted medRxiv a license to display the preprint in perpetuity. It is made available under a CC-BY 4.0 International license .

References

[1] Christophe Fraser, Steven Riley, Roy M Anderson, and Neil M Ferguson. Factors that make an infectious disease outbreak controllable. *Proceedings of the National Academy of Sciences of the United States of America*, 101(16):6146–51, apr 2004.

[2] Miriam Casey-Bryars, John Griffin, Conor Mcaloon, Andrew Byrne, Jamie Madden, David Mc, Áine Collins, Kevin Hunt, Ann Barber, Francis Butler, Elizabeth Ann Lane, Kirsty O'Brien, Patrick Wall, Kieran Walsh, and Simon John More. Presymptomatic transmission of SARS-CoV-2 infection: a secondary analysis using published data. *BMJ Open*, 11:41240, 2021.

[3] Chadi M. Saad-Roy, Ned S. Wingreen, Simon A. Levin, and Bryan T. Grenfell. Dynamics in a simple evolutionary-epidemiological model for the evolution of an initial asymptomatic infection stage. *Proceedings of the National Academy of Sciences of the United States of America*, 117(21), 2020.

[4] Chadi M. Saad-Roy, Bryan T. Grenfell, Simon A. Levin, P. Van Den Driessche, and Ned S. Wingreen. Evolution of an asymptomatic first stage of infection in a heterogeneous population. *Journal of the Royal Society Interface*, 18(179), 2021.

[5] Chadi M. Saad-Roy, Bryan T. Grenfell, Simon A. Levin, Lorenzo Pellis, Helena B. Stage, P. Van Den Driessche, and Ned S. Wingreen. Superinfection and the evolution of an initial asymptomatic stage. *Royal Society Open Science*, 8(1), 2021.

[6] S.A. Frank. Models of parasite virulence. *Quarterly Review of Biology*, 71(1):37–78, 1996.

[7] Andreas Handel and Pejman Rohani. Crossing the scale from within-host infection dynamics to between-host transmission fitness: a discussion of current assumptions and knowledge. *Philosophical Transactions of the Royal Society B*, 370(1675), 2015.

[8] Christophe Fraser, Katrina Lythgoe, Gabriel E. Leventhal, George Shirreff, T. Déirdre Hollingsworth, Samuel Alizon, and Sebastian Bonhoeffer. Virulence and pathogenesis of HIV-1 infection: An evolutionary perspective, 2014.

[9] Veasna Duong, Louis Lambrechts, Richard E Paul, Sowath Ly, Rath Srey Lay, Kanya C Long, Rekol Huy, Arnaud Tarantola, Thomas W Scott, Anavaj Sakuntabhai, and Philippe Buchy. Asymptomatic humans transmit dengue virus to mosquitoes. *Proceedings of the National Academy of Sciences of the United States of America*, 112(47):14688–93, 2015.

[10] Matthew Pollack. The role of exotoxin A in *Pseudomonas* disease and immunity. *Reviews of Infectious Diseases*, 5(S5):S979–S984, 1983.

[11] P C Turnbull, Kirsten Jorgensen, J M Kramer, R J Gilbert, and Jennifer M Parry. Severe clinical conditions associated with *Bacillus cereus* and the apparent involvement of exotoxins. *Journal of Clinical Pathology*, 32:289–293, 1979.

medRxiv preprint doi: https://doi.org/10.1101/2024.05.16.24307410; this version posted May 16, 2024. The copyright holder for this preprint (which was not certified by peer review) is the author/funder, who has granted medRxiv a license to display the preprint in perpetuity. It is made available under a CC-BY 4.0 International license .

[12] Ghassan M Matar, Fatea Ramlawi, Nabiha Hijazi, Issam Khneisser, and Alexander M Abdelnoor. Transcription levels of *Pseudomonas aeruginosa* exotoxin A gene and severity of symptoms in patients with otitis externa. *Current Microbiology*, 45:350–354, 2002.

[13] Rebecca Payne, Maximilian Muenchhoff, Jaclyn Mann, Hannah E. Roberts, Philippa Matthews, Emily Adland, Allison Hempenstall, Kuan-Hsiang Huang, Mark Brockman, Zabrina Brumme, Marc Sinclair, Toshiyuki Miura, John Frater, Myron Essex, Roger Shapiro, Bruce D. Walker, Thumbi Ndung'u, Angela R. McLean, Jonathan M. Carlson, and Philip J. R. Goulder. Impact of HLA-driven HIV adaptation on virulence in populations of high HIV seroprevalence. *Proceedings of the National Academy of Sciences*, 111:E5393–E5400, dec 2014.

[14] Daniel F. Hanson. Fever, temperature, and the immune response. *Annals of the New York Academy of Sciences*, 813(1):453–464, mar 1997.

[15] Sharon S Evans, Elizabeth A Repasky, and Daniel T Fisher. Fever and the thermal regulation of immunity: the immune system feels the heat. *Nature Reviews Immunology*, 15:335–349, 2015.

[16] Sebastian Boltaña, Sonia Rey, Nerea Roher, Reynaldo Vargas, Mario Huerta, Felicity Anne Huntingford, Frederick William Goetz, Janice Moore, Pablo Garcia-Valtanen, Amparo Estepa, and S Mackenzie. Behavioural fever is a synergic signal amplifying the innate immune response. *Proceedings of the Royal Society B: Biological Sciences*, 280, 2013.

[17] Rotem Ben-Shachar and Katia Koelle. Transmission-clearance trade-offs indicate that dengue virulence evolution depends on epidemiological context. *Nature Communications*, 9(1), 2018.

[18] Sedighe Karimzadeh, Raj Bhopal, and Nguyen Tien Huy. Review of infective dose, routes of transmission and outcome of COVID-19 caused by the SARS-COV-2: comparison with other respiratory viruses. *Epidemiology and Infection*, 149(e96):1–8, 2021.

[19] Zuzana Střížová, Jiřina Bartůňková, and Daniel Smrž. Can wearing face masks in public affect transmission route and viral load in COVID-19? *Central European Journal of Public Health*, 28(2):161–162, 2020.

[20] Stephen Burgess, David Smith, Julia C Kenyon, and Dipender Gill. Lightening the viral load to lessen covid-19 severity. *The BMJ*, 371, 2020.

[21] Ana Filipovic, Ehsan Ghasemian, Aleksandra Inic-Kanada, Ivana Lukic, Elisabeth Stein, Emilija Marinkovic, Radmila Djokic, Dejana Kosanovic, Nadine Schuerer, Hadeel Chalabi, Sandra Belij-Rammerstorfer, Marijana Stojanovic, and Talin Barisani-Asenbauer. The effect of infectious dose on humoral and cellular immune responses in *Chlamydophila caviae* primary ocular infection. *PLOS ONE*, 12(7):e0180551, jul 2017.

[22] João Alves Gama, Sophie S. Abby, Sara Vieira-Silva, Francisco Dionisio, and Eduardo P. C. Rocha. Immune subversion and quorum-sensing shape the variation in infectious dose among bacterial pathogens. *PLOS Pathogens*, 8(2):e1002503, feb 2012.

medRxiv preprint doi: https://doi.org/10.1101/2024.05.16.24307410; this version posted May 16, 2024. The copyright holder for this preprint (which was not certified by peer review) is the author/funder, who has granted medRxiv a license to display the preprint in perpetuity. It is made available under a CC-BY 4.0 International license .

[23] Andrew J Pollard, Julian Savulescu, John Oxford, Adrian VS Hill, Myron M Levine, David JM Lewis, Robert C Read, David Y Graham, Wellington Sun, Peter Openshaw, and Stephen B Gordon. Human microbial challenge: the ultimate animal model. *The Lancet Infectious Diseases*, 12(12):903–905, 2012.

[24] Meta Roestenberg, Marie-Astrid Hoogerwerf, Daniela M Ferreira, Benjamin Mordmüller, and Maria Yazdanbakhsh. Experimental infection of human volunteers. *The Lancet Infectious Diseases*, 18(10):e312–e322, 2018.

[25] A. E. Kirby, J. Shi, J. Montes, M. Lichtenstein, and C. L. Moe. Disease course and viral shedding in experimental Norwalk virus and Snow Mountain virus infection. *Journal of Medical Virology*, 86(12):2055–2064, dec 2014.

[26] Bindiya Bagga, Christopher W. Woods, Timothy H. Veldman, Anthony Gilbert, Alex Mann, Ganesh Balaratnam, Robert Lambkin-Williams, John S. Oxford, Micah T. McClain, Tom Wilkinson, Brad P. Nicholson, Geoffrey S. Ginsburg, and John P. DeVincenzo. Comparing inluenza and RSV viral and disease dynamics in experimentally infected adults predicts clinical effectiveness of RSV antivirals. *Antiviral Therapy*, 18(6):785–791, 2013.

[27] R. G. Douglas and R. F. Betts. Effect of induced interferon in experimental rhinovirus infections in volunteers. *Infection and Immunity*, 9(3):506–510, 1974.

[28] Robert L. Atmar, Antone R. Opekun, Mark A. Gilger, Mary K. Estes, Sue E. Crawford, Frederick H. Neill, and David Y. Graham. Norwalk virus shedding after experimental human infection. *Emerging Infectious Diseases*, 14(10):1553–1557, oct 2008.

[29] Yan Li and Andreas Handel. Modeling inoculum dose dependent patterns of acute virus infections. *Journal of Theoretical Biology*, 347(1):63–73, apr 2014.

[30] Aaron A. King, Sourya Shrestha, Eric T. Harvill, and Ottar N. Bjørnstad. Evolution of acute infections and the invasion-persistence trade-off. *The American naturalist*, 173(4):446, apr 2009.

[31] Ben Killingley, Alex J. Mann, Mariya Kalinova, Alison Boyers, Niluka Goonawardane, Jie Zhou, Kate Lindsell, Samanjit S. Hare, Jonathan Brown, Rebecca Frise, Emma Smith, Claire Hopkins, Nicolas Noulin, Brandon Löndt, Tom Wilkinson, Stephen Harden, Helen McShane, Mark Baillet, Anthony Gilbert, Michael Jacobs, Christine Charman, Priya Mande, Jonathan S. Nguyen-Van-Tam, Malcolm G. Semple, Robert C. Read, Neil M. Ferguson, Peter J. Openshaw, Garth Rapeport, Wendy S. Barclay, Andrew P. Catchpole, and Christopher Chiu. Safety, tolerability and viral kinetics during SARS-CoV-2 human challenge in young adults. *Nature Medicine*, 28:1031–1041, mar 2022.

[32] John DeVincenzo, Dereck Tait, John Efthimiou, Julie Mori, Young In Kim, Elaine Thomas, Lynn Wilson, Rachel Harland, Neil Mathews, Stuart Cockerill, Kenneth Powell, and Edward Littler. A randomized, placebo-controlled, respiratory syncytial virus human challenge study of the antiviral efficacy, safety, and pharmacokinetics of RV521,

medRxiv preprint doi: https://doi.org/10.1101/2024.05.16.24307410; this version posted May 16, 2024. The copyright holder for this preprint (which was not certified by peer review) is the author/funder, who has granted medRxiv a license to display the preprint in perpetuity. It is made available under a CC-BY 4.0 International license .

an inhibitor of the RSV-F protein. *Antimicrobial Agents and Chemotherapy*, 64(2), jan 2020.

[33] John P. DeVincenzo, Tom Wilkinson, Akshay Vaishnaw, Jeff Cehelsky, Rachel Meyers, Saraswathy Nochur, Lisa Harrison, Patricia Meeking, Alex Mann, Elizabeth Moane, John Oxford, Rajat Pareek, Ryves Moore, Ed Walsh, Robert Studholme, Preston Dorsett, Rene Alvarez, and Robert Lambkin-Williams. Viral load drives disease in humans experimentally infected with respiratory syncytial virus. *American Journal of Respiratory and Critical Care Medicine*, 182(10):1305–1314, nov 2010.

[34] Scherer P Sanders, David Proud, Solbert Permutt, Edward S Siekierski, Robin Yachechko, and Mark C Liu. Role of nasal nitric oxide in the resolution of experimental rhinovirus infection. *Journal of Allergy and Clinical Immunology*, 113(4):697–702, 2004.

[35] F. G. Hayden, K. Andries, and P. A.J. Janssen. Safety and efficacy of intranasal pirodavir (R77975) in experimental rhinovirus infection. *Antimicrobial Agents and Chemotherapy*, 36(4):727–732, 1992.

[36] L. Mark Gustafson, David Proud, J. Owen Hendley, Frederick G. Hayden, and Jack M. Gwaltney Jr. Oral prednisone therapy in experimental rhinovirus infections. *Journal of Allergy and Clinical Immunology*, 97:1009–1014, 1996.

[37] David I Bernstein, Robert L Atmar, G Marshall Lyon, John J Treanor, Wilbur H Chen, Xi Jiang, Jan Vinjé, Nicole Gregoricus, Robert W Frenck, Christine L Moe, Mohamed S Al-Ibrahim, Jill Barrett, Jennifer Ferreira, Mary K Estes, David Y Graham, Robert Goodwin, Astrid Borkowski, Ralf Clemens, and Paul M Mendelman. Norovirus vaccine against experimental human G11.4 virus illness: A challenge study in healthy adults. *The Journal of Infectious Diseases*, 211(6):870–878, 2015.

[38] Robert L. Atmar, David I. Bernstein, Clayton D. Harro, Mohamed S. Al-Ibrahim, Wilbur H. Chen, Jennifer Ferreira, Mary K. Estes, David Y. Graham, Antone R. Opekun, Charles Richardson, and Paul M. Mendelman. Norovirus vaccine against experimental human Norwalk virus illness. *New England Journal of Medicine*, 365(23):2178–2187, dec 2011.

[39] Frederick G. Hayden, Lance. Jennings, Richard. Robson, Gilbert. Schiff, Helen. Jackson, Brinderjeet. Rana, Graham. McClelland, David. Ipe, Noel. Roberts, and Penelope. Ward. Oral oseltamivir in human experimental influenza B infection. *Antiviral Therapy*, 5(3):205–213, 2000.

[40] Luis. Barroso, John J. Treanor, Larisa. Gubareva, and Frederick G. Hayden. Efficacy and tolerability of the oral neuraminidase inhibitor peramivir in experimental human influenza: Randomized, controlled trials for prophylaxis and treatment. Technical report, 2005.

[41] M T Mcclain, R Henao, J Williams, B Nicholson, T Veldman, L Hudson, E L Tsalik, R Lambkin-Williams, A Gilbert, A Mann, G S Ginsburg, and C W Woods. Differential evolution of peripheral cytokine levels in symptomatic and asymptomatic re-

medRxiv preprint doi: https://doi.org/10.1101/2024.05.16.24307410; this version posted May 16, 2024. The copyright holder for this preprint (which was not certified by peer review) is the author/funder, who has granted medRxiv a license to display the preprint in perpetuity. It is made available under a CC-BY 4.0 International license .

sponses to experimental influenza virus challenge. *Clinical and Experimental Immunology*, 183(3):441–451, 2016.

[42] Justin R Ortiz, David I Bernstein, Daniel F Hoft, Christopher W Woods, Micah T Mcclain, Sharon E Frey, Rebecca C Brady, Christopher Bryant, Ashley Wegel, Robert W Frenck, Emmanuel B Walter, Getahun Abate, Sarah R Williams, Robert L Atmar, Wendy A Keitel, Nadine Rouphael, Mathew J Memoli, Mamodikoe K Makhene, Paul C Roberts, and Kathleen M Neuzil. A multicenter, controlled human infection study of influenza A(H1N1)pdm09 in healthy adults. *The Journal of Infectious Diseases*, 228(3):287–298, 2023.

[43] Jacqueline M. McBride, Jeremy J. Lim, Tracy Burgess, Rong Deng, Michael A. Derby, Mauricio Maia, Priscilla Horn, Omer Siddiqui, Daniel Sheinson, Haiyin Chen-Harris, Elizabeth M. Newton, Dimitri Fillos, Denise Nazzal, Carrie M. Rosenberger, Maikke B. Ohlson, Rob Lambkin-Williams, Hosnieh Fathi, Jeffrey M. Harris, and Jorge A. Tavela. Phase 2 randomized trial of the safety and efficacy of MHAA4549A, a broadly neutralizing monoclonal antibody, in a human influenza a virus challenge model. *Antimicrobial Agents and Chemotherapy*, 61(11), oct 2017.

[44] Larisa V Gubareva, Laurent Kaiser, Mikhail N Matrosovich, Yee Soo-Hoo, and Frederick G Hayden. Selection of influenza virus mutants in experimentally infected volunteers treated with Oseltamivir. *The Journal of Infectious Diseases*, 183(4):523–531, 2001.

[45] Jeannette M. Watson, James N. Francis, Sofie Mesens, Gabriel A. Faiman, Jill Makin, Peter Patriarca, John J. Treanor, Bertrand Georges, and Campbell J. Bunce. Characterisation of a wild-type influenza (A/H1N1) virus strain as an experimental challenge agent in humans. *Virology Journal*, 12, feb 2015.

[46] Jose M. Trevejo, Mohammed Asmal, Johan Vingerhoets, Ramon Polo, Sarah Robertson, Ying Jiang, Tara L. Kieffer, and Lorant Leopold. Pimodivir treatment in adult volunteers experimentally inoculated with live influenza virus: A phase IIa, randomized, double-blind, placebo-controlled study. *Antiviral Therapy*, 23(4):335–344, 2018.

[47] David P. Calfee, Amy W. Peng, Lindsey M. Cass, Monica Lobo, and Frederick G. Hayden. Safety and efficacy of intravenous zanamivir in preventing experimental human influenza A virus infection. *Antimicrobial Agents and Chemotherapy*, 43(7):1616–1620, 1999.

[48] R. Scott Fritz, Frederick G. Hayden, David P. Calfee, Lindsey M.R. Cass, Amy W. Peng, W. Gregory Alvord, Warren Strober, and Stephen E. Straus. Nasal cytokine and chemokine responses in experimental influenza A virus infection: Results of a placebo-controlled trial of intravenous zanamivir treatment. *Journal of Infectious Diseases*, 180(3):586–593, sep 1999.

[49] Laurent Kaiser, Marcus S. Briones, and Frederick G. Hayden. Performance of virus isolation and Directigen® Flu A to detect influenza A virus in experimental human infection. *Journal of Clinical Virology*, 14(3):191–197, dec 1999.

medRxiv preprint doi: https://doi.org/10.1101/2024.05.16.24307410; this version posted May 16, 2024. The copyright holder for this preprint (which was not certified by peer review) is the author/funder, who has granted medRxiv a license to display the preprint in perpetuity. It is made available under a CC-BY 4.0 International license .

[50] S. D. Sears and M. L. Clements. Protective efficacy of low-dose amantadine in adults challenged with wild-type influenza A virus. *Antimicrobial Agents and Chemotherapy*, 31(10):1470–1473, 1987.

[51] C. R. Magnussen, R. G. Douglas, R. F. Betts, F. K. Roth, and M. P. Meagher. Double-blind evaluation of oral ribavirin (virazole) in experimental influenza A virus infection in volunteers. *Antimicrobial Agents and Chemotherapy*, 12(4):498–502, 1977.

[52] Andrew W. Murphy, Thomas A.E. Platts-Mills, Monica Lobo, and Frederick Hayden. Respiratory nitric oxide levels in experimental human influenza. *Chest*, 114(2):452–456, aug 1998.

[53] Frederick G. Hayden, R. Scott Fritz, Monica C. Lobo, W. Gregory Alvord, Warren Strober, and Stephen E. Straus. Local and systemic cytokine responses during experimental human influenza A virus infection. Relation to symptom formation and host defense. *Journal of Clinical Investigation*, 101(3):643–649, feb 1998.

[54] Kuan Ying Arthur Huang, Chris Ka Fai Li, Elizabeth Clutterbuck, Cecilia Chui, Tom Wilkinson, Anthony Gilbert, John Oxford, Rob Lambkin-Williams, Tzou Yien Lin, Andrew J. Mcmichael, and Xiao Ning Xu. Virus-specific antibody secreting cell, memory B-cell, and sero-antibody responses in the human influenza challenge model. *Journal of Infectious Diseases*, 209(9):1354–1361, may 2014.

[55] Alison Han, Lindsay M. Czajkowski, Amanda Donaldson, Holly Ann Baus, Susan M. Reed, Rani S. Athota, Tyler Bristol, Luz Angela Rosas, Adriana Cervantes-Medina, Jeffery K. Taubenberger, and Matthew J. Memoli. A dose-finding study of a wild-type influenza A(H3N2) virus in a healthy volunteer human challenge model. *Clinical Infectious Diseases*, 69(12):2082–2090, nov 2019.

[56] Paul Jacob Bueno de Mesquita, Jonathan Nguyen-Van-Tam, Ben Killingley, Joanne Enstone, Robert Lambkin-Williams, Anthony S. Gilbert, Alexander Mann, John Forni, Jing Yan, Jovan Pantelic, Michael L. Grantham, and Donald K. Milton. Influenza A (H3) illness and viral aerosol shedding from symptomatic naturally infected and experimentally infected cases. *Influenza and other Respiratory Viruses*, 15(1):154–163, jan 2020.

[57] Nicola Procházková, Gwen Falony, Lars Ove Dragsted, Tine Rask Licht, Jeroen Raes, and Henrik M. Roager. Advancing human gut microbiota research by considering gut transit time. *Gut*, 72(1):180–191, 2023.

[58] Yu Wang, Huaiyu Tian, Li Zhang, Man Zhang, Dandan Guo, Wenting Wu, Xingxing Zhang, Ge Lin Kan, Lei Jia, Da Huo, Baiwei Liu, Xiaoli Wang, Ying Sun, Quanyi Wang, Peng Yang, and C Raina Macintyre. Reduction of secondary transmission of SARS-CoV-2 in households by face mask use, disinfection and social distancing: a cohort study in Beijing, China. *BMJ Global Health*, 5:2794, 2020.

[59] Xiang Ren, Yu Li, Xiaokun Yang, Zhili Li, Jinzhao Cui, Aiqin Zhu, Hongting Zhao, Jianxing Yu, Taoran Nie, Minrui Ren, Shuaibing Dong, Ying Cheng, Qiulan Chen,

medRxiv preprint doi: https://doi.org/10.1101/2024.05.16.24307410; this version posted May 16, 2024. The copyright holder for this preprint (which was not certified by peer review) is the author/funder, who has granted medRxiv a license to display the preprint in perpetuity. It is made available under a CC-BY 4.0 International license .

Zhaorui Chang, Junling Sun, Liping Wang, Luzhao Feng, George F Gao, Zijian Feng, and Zhongjie Li. Evidence for pre-symptomatic transmission of coronavirus disease 2019 (COVID-19) in China. *Influenza and other Respiratory Viruses*, 15(1):19–26, 2021.

[60] Muge Cevik, Matthew Tate, Ollie Lloyd, Alberto Enrico Maraolo, Jenna Schafers, and Antonia Ho. SARS-CoV-2, SARS-CoV, and MERS-CoV viral load dynamics, duration of viral shedding, and infectiousness: a systematic review and meta-analysis. *The Lancet Microbe*, 2(1):e13–e22, jan 2021.

[61] Zhonglan Wu, David Harrich, Zhongyang Li, Dongsheng Hu, and Dongsheng Li. The unique features of SARS-CoV-2 transmission: Comparison with SARS-CoV, MERS-CoV and 2009 H1N1 pandemic influenza virus. *Reviews in Medical Virology*, 31(2):1–11, 2021.

[62] Jordi Ripoll and Jordi Font. A discrete model for the evolution of infection prior to symptom onset. *Mathematics*, 11, 2 2023.

[63] James J. Bull and Adam S. Lauring. Theory and empiricism in virulence evolution. *PLoS Pathogens*, 10(10), 2014.

[64] Megan A Greischar, Lindsay M Beck-Johnson, and Nicole Mideo. Partitioning the influence of ecology across scales on parasite evolution. *Evolution*, 2019.

[65] Damie Pak, Tsukushi Kamiya, and Megan A. Greischar. Proliferation in malaria parasites: how resource limitation can prevent evolution of greater virulence. *bioRxiv*, 2023.

[66] Troy Day. Virulence evolution and the timing of disease life-history events. *Trends in Ecology & Evolution*, 18(3):113–118, 2003.

[67] Chia C. Wang, Kimberly A. Prather, Josué Sznitman, Jose L. Jimenez, Seema S. Lakdawala, Zeynep Tufekci, and Linsey C. Marr. Airborne transmission of respiratory viruses. *Science*, 373(6558), 2021.

[68] F. Ellis McKenzie, David L. Smith, Wendy P. O'Meara, and Eleanor M. Riley. Chapter 1 strain theory of malaria: The first 50 years. *Advances in Parasitology*, 66:1–46, 2008.

[69] Isabelle Marois, Alexandre Cloutier, Émilie Garneau, and Martin V Richter. Initial infectious dose dictates the innate, adaptive, and memory responses to influenza in the respiratory tract. *Journal of Leukocyte Biology*, 92(1):107–121, 2012.

[70] Aaron Nicholas Gillman, Anel Mahmutovic, Pia Abel zur Wiesch, and Sören Abel. The infectious dose shapes *Vibrio cholerae* within-host dynamics. *mSystems*, 6(6), 2021.

[71] Paul A. Dabisch, Jennifer Biryukov, Katie Beck, Jeremy A. Boydston, Jaleal S. Sanjak, Artemas Herzog, Brian Green, Gregory Williams, John Yeager, Jordan K. Bohannon, Brian Holland, David Miller, Amy L. Reese, Denise Freeburger, Susan Miller, Tammy Jenkins, Sherry Rippeon, James Miller, David Clarke, Emmanuel Manan, Ashley Patty, Kim Rhodes, Tina Sweeney, Michael Winpigler, Owen Price, Jason Rodriguez, Louis A.

medRxiv preprint doi: https://doi.org/10.1101/2024.05.16.24307410; this version posted May 16, 2024. The copyright holder for this preprint (which was not certified by peer review) is the author/funder, who has granted medRxiv a license to display the preprint in perpetuity. It is made available under a CC-BY 4.0 International license .

Altamura, Heather Zimmerman, Alec S. Hail, Victoria Wahl, and Michael Hevey. Seroconversion and fever are dosepependent in a nonhuman primate model of inhalational COVID-19. *PLoS Pathogens*, 17(8):1–19, 2021.

[72] Madeline G. Douglas, Jacob F. Kocher, Trevor Scobey, Ralph S. Baric, and Adam S. Cockrell. Adaptive evolution influences the infectious dose of MERS-CoV necessary to achieve severe respiratory disease. *Virology*, 517(September 2017):98–107, 2018.

[73] Alfredo Alberti, Liliana Chemello, and Luisa Benvegnù. Natural history of hepatitis C. *Journal of Hepatology, Supplement*, 31(1):17–24, 1999.

[74] Franck Courchamp, Luděk Berec, and Joanna Gascoigne. *Allee effects in ecology and conservation*. Oxford University Press, New York, 2008.

[75] C. J. E. Metcalf, A. L. Graham, S. Huijben, V. C. Barclay, G. H. Long, B. T. Grenfell, a. F. Read, and O. N. Bjørnstad. Supplement: partitioning regulatory mechanisms of within-host malaria dynamics using the effective propagation number. *Science*, 333(6045):984–988, aug 2011.

[76] Anca Dorhoi, Stephen T. Reece, and Stefan H.E. Kaufmann. For better or for worse: The immune response against *Mycobacterium tuberculosis* balances pathology and protection. *Immunological Reviews*, 240(1):235–251, 2011.

[77] Varvara A. Ryabkova, Leonid P. Churilov, and Yehuda Shoenfeld. Influenza infection, SARS, MERS and COVID-19: Cytokine storm – The common denominator and the lessons to be learned. *Clinical Immunology*, 223(November 2020):108652, 2021.

[78] Brian Imbiakha, Julie M. Sahler, David W. Buchholz, Shahrzad Ezzatpour, Mason Jager, Annette Choi, Isaac A. Monreal, Haewon Byun, Richard Ayomide Adeleke, Justin Leach, Gary Whittaker, Stephen Dewhurst, Brian D. Rudd, Hector C. Aguilar, and Avery August. Adaptive immune cells are necessary for SARS-CoV-2–induced pathology. *Science Advances*, 10(1), 2024.

[79] Lin-Man Weng, Xuan Su, and Xue-Qiang Wang. Pain symptoms in patients with coronavirus disease (COVID-19): A literature review. *Journal of Pain Research*, 14:147–159, 2022.

[80] Andrea Mastrangelo, Matteo Bonato, and Paola Cinque. Smell and taste disorders in COVID-19: From pathogenesis to clinical features and outcomes. *Neuroscience Letters*, 748, mar 2021.

[81] J O Lloyd-Smith, S J Schreiber, P E Kopp, and W M Getz. Superspreading and the effect of individual variation on disease emergence. *Nature*, 438(7066):355–9, nov 2005.

[82] Joel L. Pick, Shinichi Nakagawa, and Daniel W.A. Noble. Reproducible, flexible and high-throughput data extraction from primary literature: The metaDigitise R package. *Methods in Ecology and Evolution*, 10(3):426–431, 2018.

medRxiv preprint doi: https://doi.org/10.1101/2024.05.16.24307410; this version posted May 16, 2024. The copyright holder for this preprint (which was not certified by peer review) is the author/funder, who has granted medRxiv a license to display the preprint in perpetuity. It is made available under a CC-BY 4.0 International license .

Supplemental figures & table

Parameter	Value
Pathogen replication rate (r)	10-250
Immune cell kill rate (k)	3.5
Basal immune cell birth rate (α)	1
Immune cell death rate (d)	0.5
Immune cell recruitment rate (γ)	10^{-4}

Table 1: Ranges for model parameters.

medRxiv preprint doi: https://doi.org/10.1101/2024.05.16.24307410; this version posted May 16, 2024. The copyright holder for this preprint (which was not certified by peer review) is the author/funder, who has granted medRxiv a license to display the preprint in perpetuity. It is made available under a CC-BY 4.0 International license .

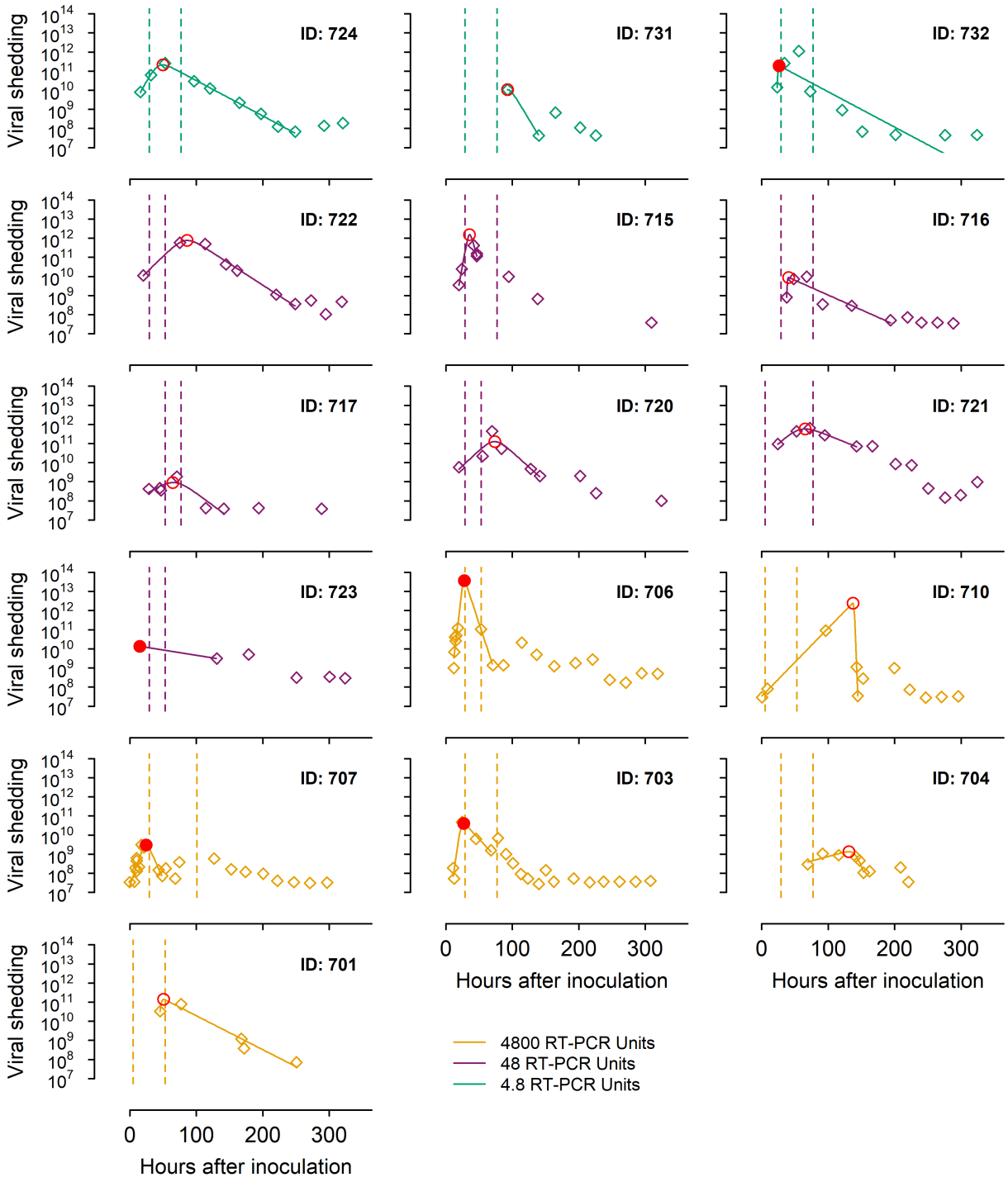

Figure S1: One participant from the group inoculated with an infectious dose of 4.8 RT-PCR units and three from the group inoculated with a dose of 4800 RT-PCR units demonstrate pre-symptomatic transmission [28]. The dots indicate viral shedding, the solid line indicates the fit of Equation 1, and the dotted vertical lines indicate the onset and end of symptoms. The infectious dose and whether the participant experienced pre-symptomatic or post-symptomatic transmission are indicated at the top of each plot. The viral shedding trajectory model was fit from the first observed viral shedding value to the first local minimum after peak viral shedding. Participants 723 and 731 were excluded from subsequent analyses due to unclear peaks.

medRxiv preprint doi: https://doi.org/10.1101/2024.05.16.24307410; this version posted May 16, 2024. The copyright holder for this preprint (which was not certified by peer review) is the author/funder, who has granted medRxiv a license to display the preprint in perpetuity. It is made available under a CC-BY 4.0 International license .

[!h]

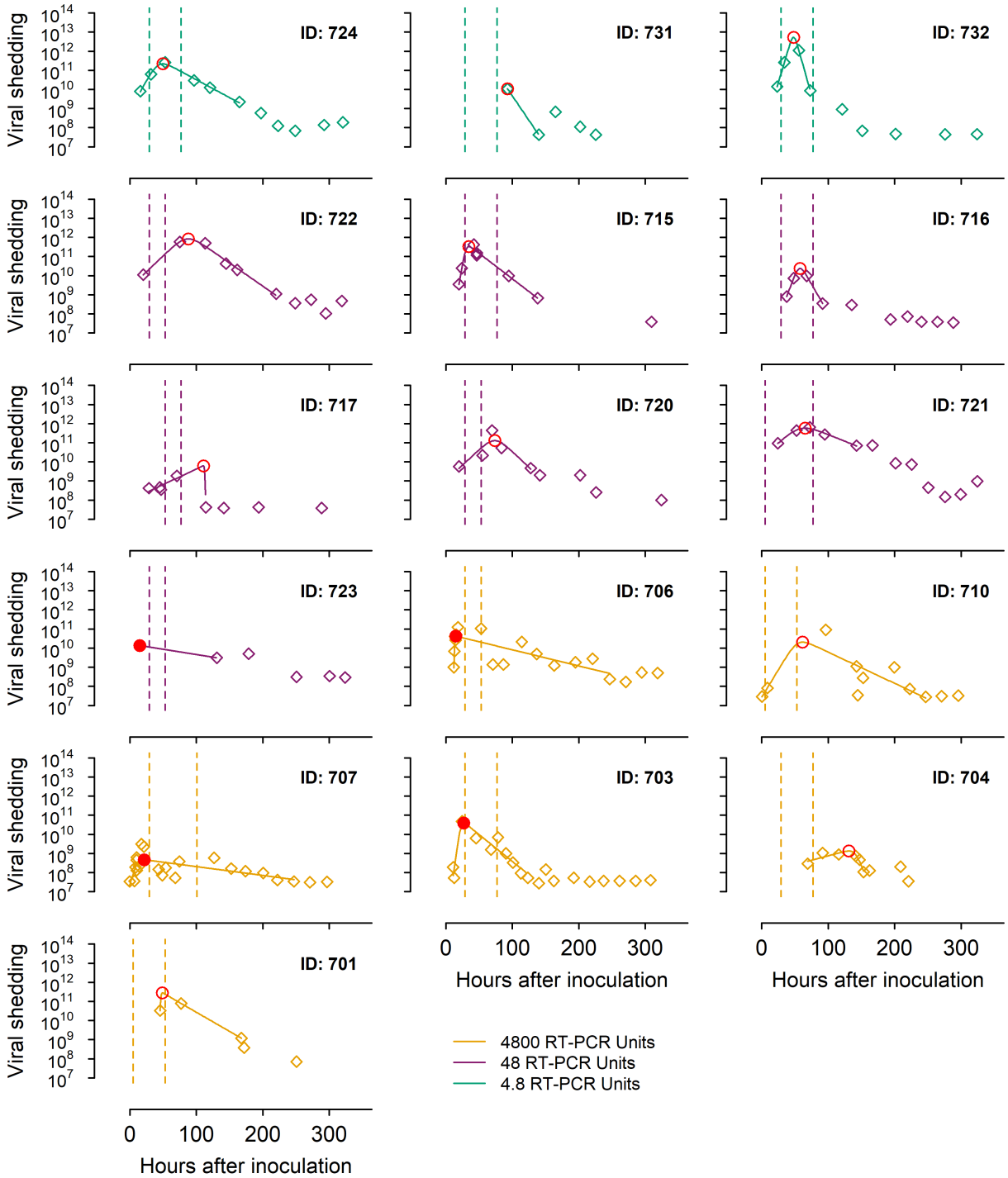

Figure S2: Viral shedding trajectory of participants from [28] using an alternate criterion for the endpoint. The dots indicate viral shedding, the solid line indicates the fit of Equation 1, and the dotted vertical lines indicate the onset and end of symptoms. The infectious dose and whether the participant experienced pre-symptomatic or post-symptomatic transmission are indicated at the top of each plot. The trajectory model was fit from the first observed viral shedding value to the first value after peak viral shedding that is less than or equal to the first observed viral shedding value.

medRxiv preprint doi: https://doi.org/10.1101/2024.05.16.24307410; this version posted May 16, 2024. The copyright holder for this preprint (which was not certified by peer review) is the author/funder, who has granted medRxiv a license to display the preprint in perpetuity. It is made available under a CC-BY 4.0 International license .

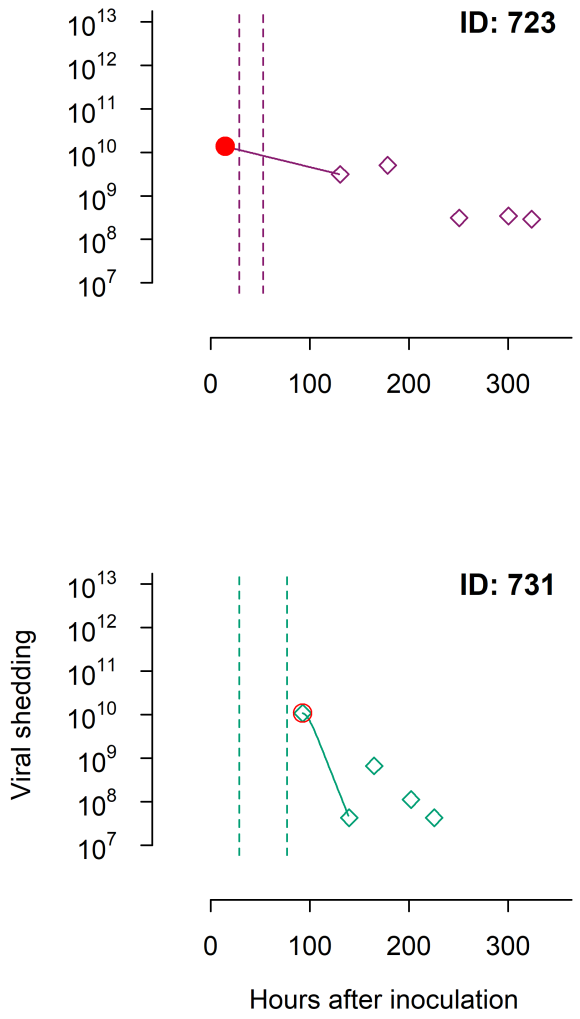

Figure S3: Two participants from [28] were disqualified from our analyses due to lacking a clear pathogen shedding peak: participants 723 and 731.

medRxiv preprint doi: https://doi.org/10.1101/2024.05.16.24307410; this version posted May 16, 2024. The copyright holder for this preprint (which was not certified by peer review) is the author/funder, who has granted medRxiv a license to display the preprint in perpetuity. It is made available under a CC-BY 4.0 International license .

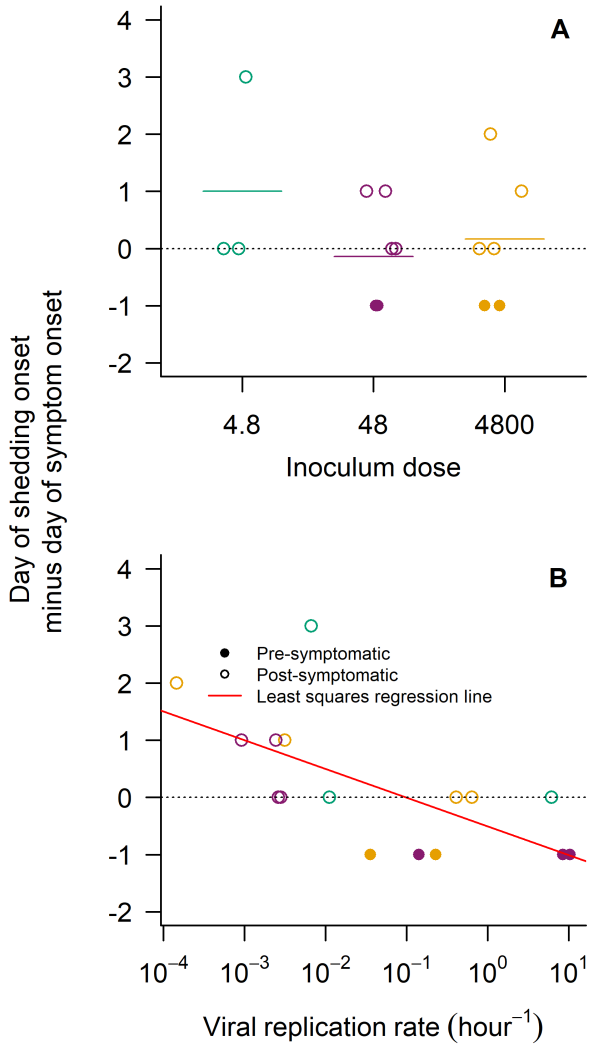

Figure S4: Norovirus data [28] exhibit no dose-dependence in the relative timing of symptom and shedding onset, but do demonstrate a positive correlation between viral replication rate and pre-symptomatic transmission. Panel A shows the delay between symptom and shedding onset for each patient, comparing across infectious dose, with horizontal bars to indicate the average delay for each dose. Panel B shows that the delay between symptom onset and shedding onset becomes more negative with faster estimated viral replication rate (P_2, Eq. 1). As viral replication rate increases, it is more likely that shedding onset will precede symptom onset ($p = 0.0064$).

medRxiv preprint doi: https://doi.org/10.1101/2024.05.16.24307410; this version posted May 16, 2024. The copyright holder for this preprint (which was not certified by peer review) is the author/funder, who has granted medRxiv a license to display the preprint in perpetuity. It is made available under a CC-BY 4.0 International license .

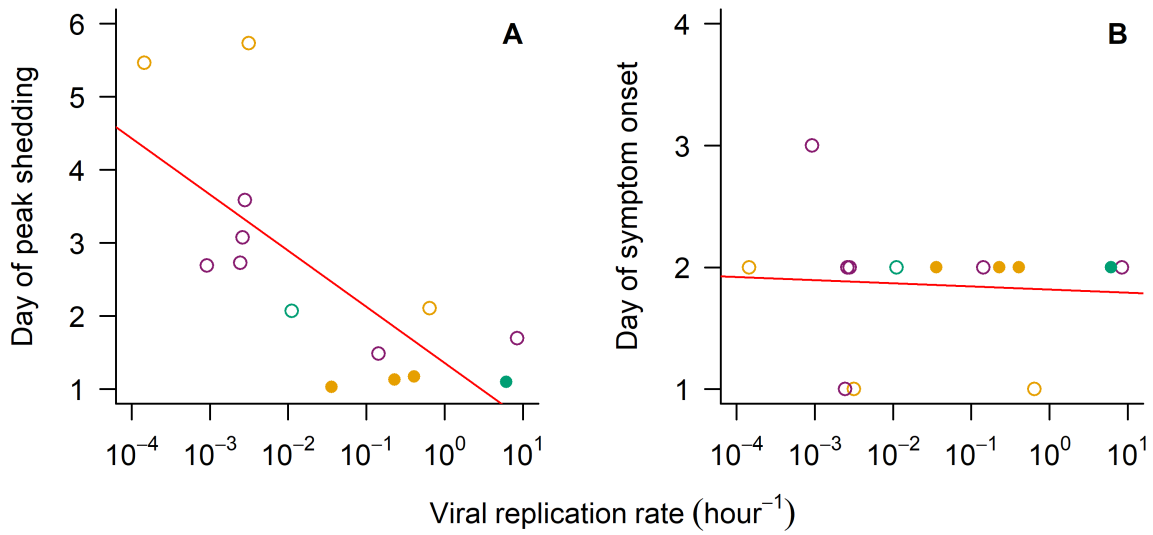

Figure S5: The correlation between pre-symptomatic transmission and pathogen replication rate (as approximated by P_2 from Equation 1) is mostly a product of the negative correlation between the timing of peak shedding and pathogen replication rate. The faster the pathogen replicates, the earlier an individual's shedding peaks ($p = 0.0029$). There is no significant correlation between the timing of symptom onset and pathogen replication rate ($p = 0.8125$).

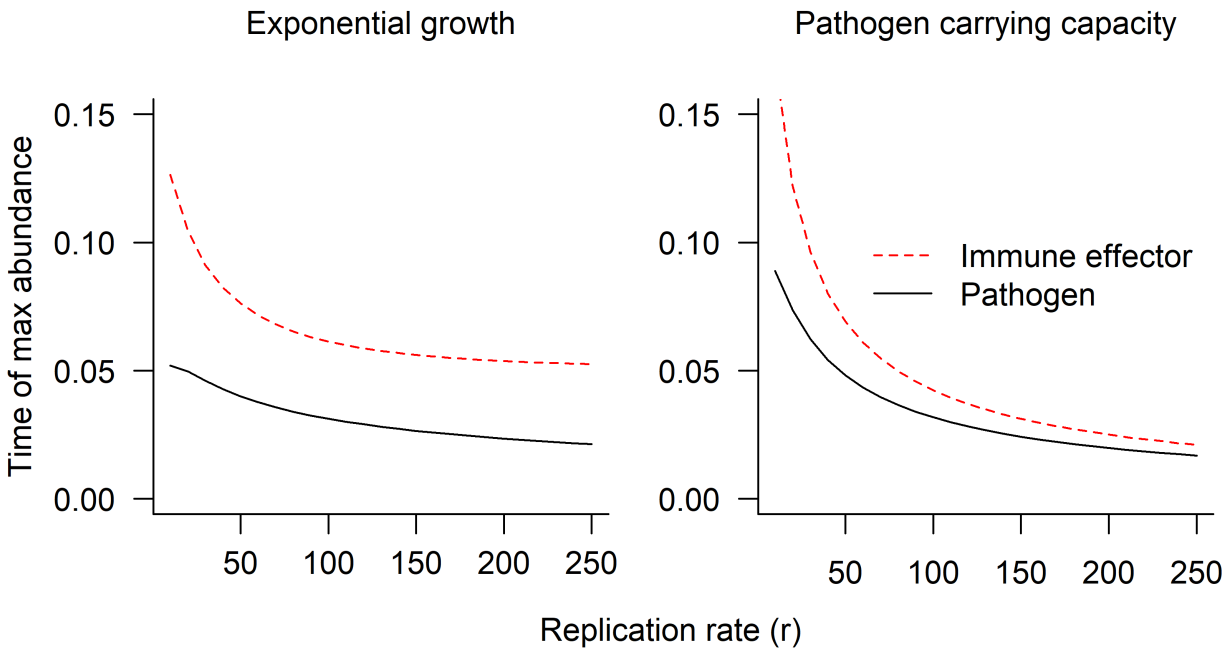

Figure S6: Immune response (X) peaks after pathogen load (P) in our mechanistic model (Equations 2 and 3) across all of the pathogen replication rates we used ($r = 10$ to 250 by increments of 10).

medRxiv preprint doi: https://doi.org/10.1101/2024.05.16.24307410; this version posted May 16, 2024. The copyright holder for this preprint (which was not certified by peer review) is the author/funder, who has granted medRxiv a license to display the preprint in perpetuity. It is made available under a CC-BY 4.0 International license .

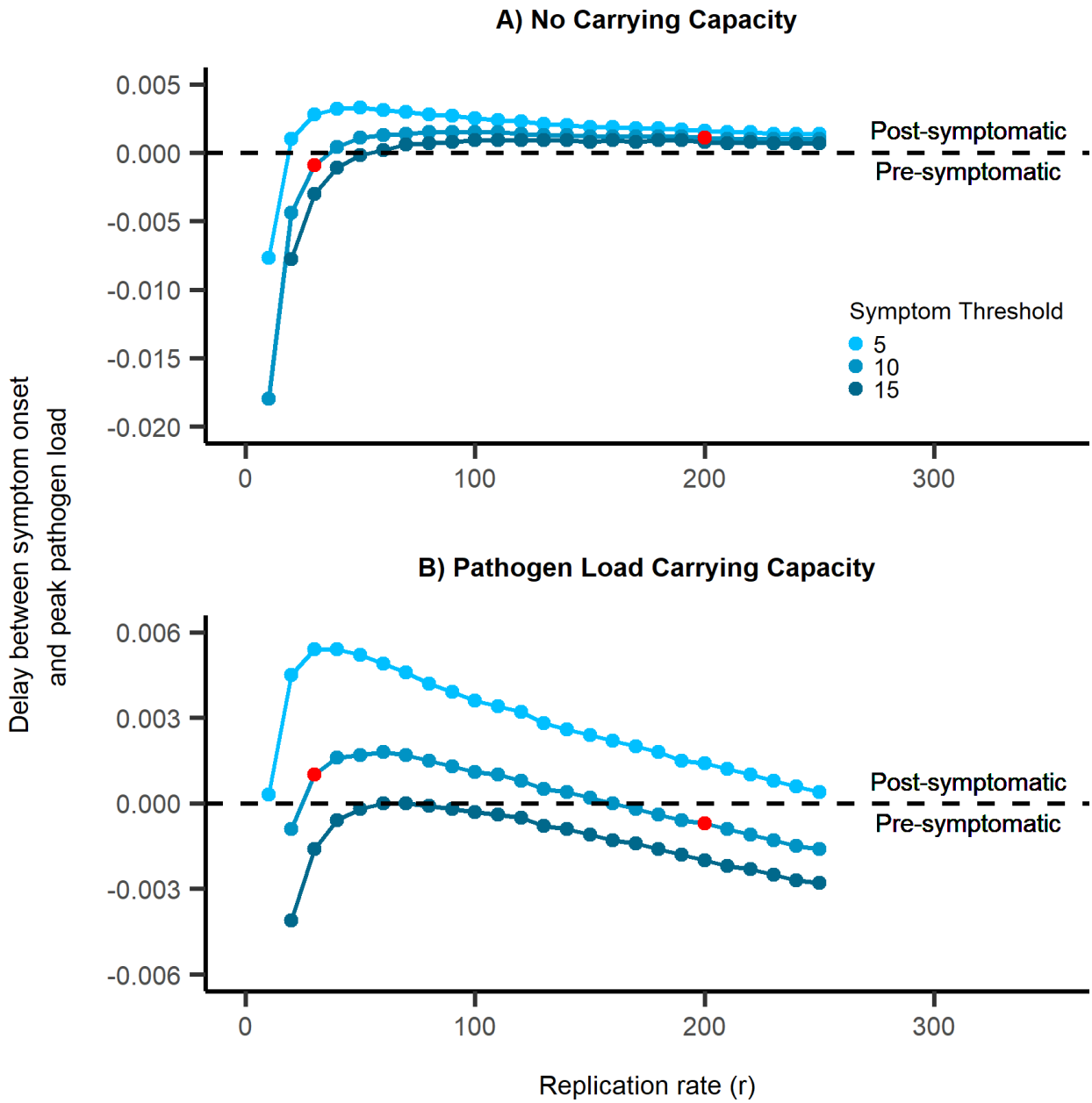

Figure S7: Assumptions about whether pathogen growth is exponential or limited by a carrying capacity change the relationship between replication rate and pre-symptomatic transmission. Both models shown here assume that symptom onset occurs when immune effector abundance exceeds an arbitrary threshold s_X. In the model with exponential pathogen growth (Equations 2, 3, and 5 where $\eta = 1$), a higher pathogen replication rate (r) decreases the chance of pre-symptomatic transmission (A). With a carrying capacity ($\theta = 5 \times 10^5$), faster replication first reduces then increases pre-symptomatic transmission. Other parameters set are as follows: immune cell kill rate, $k = 3.5$ (A) and $k = 7$ (B); immune response recruitment rate, $\gamma = 10^{-4}$; immune cell birth rate, $\alpha = 1$; immune cell death rate, $d = 0.5$; and initial pathogen dose, $P(0) = 10^5$. Symptom thresholds s_X from low to high are 5, 10, and 15 for panel A and 1, 2, 3 for panel B. The replication rates used in Fig. 4B, C are highlighted in red.

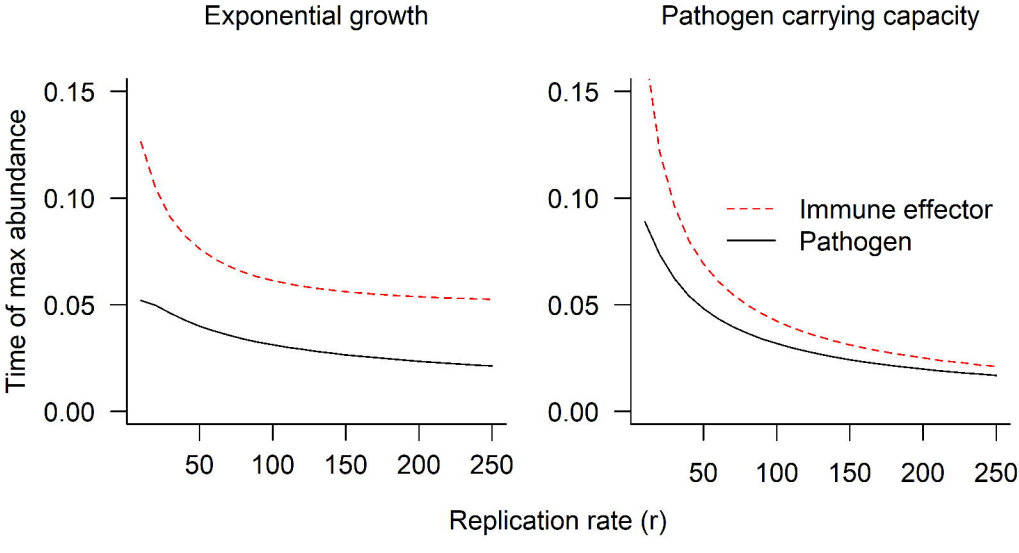
Exponential growth
Pathogen carrying capacity
Time of max abundance
0.15
0.10
0.05
0.00
50
100
150
200
250
Immune effector
Pathogen
Replication rate (r)

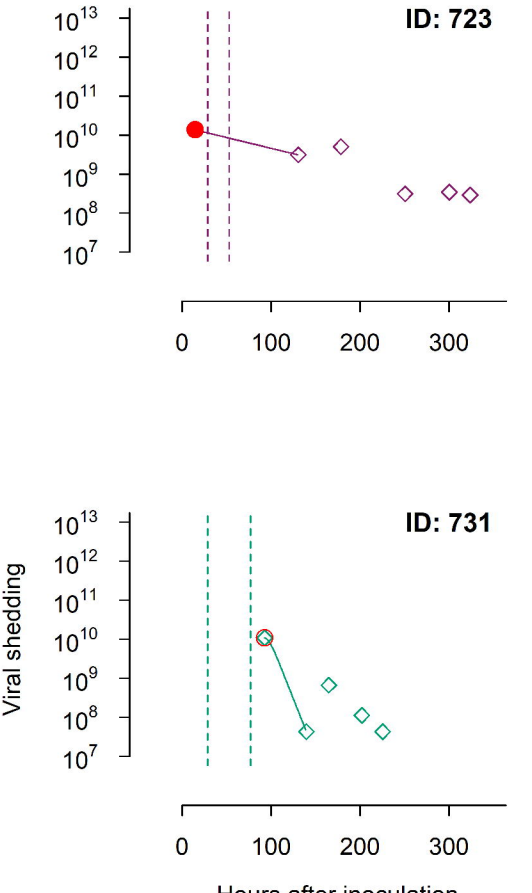
ID: 723
ID: 731
Viral shedding
10^{13}
10^{12}
10^{11}
10^{10}
10^{9}
10^{8}
10^{7}
0
100
200
300
Hours after inoculation

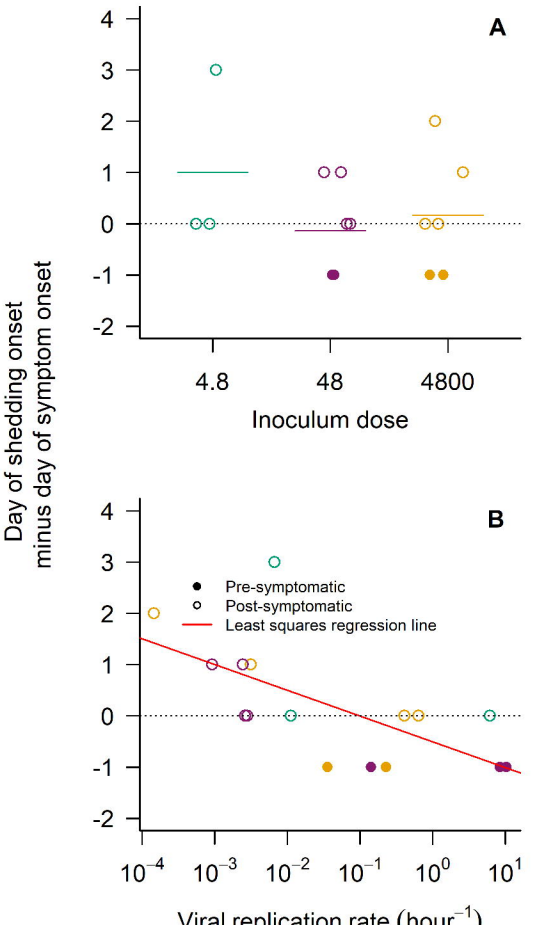
A
B
Day of shedding onset
minus day of symptom onset
4
3
2
1
0
-1
-2
4.8
48
4800
Inoculum dose
Pre-symptomatic
Post-symptomatic
Least squares regression line
10^{-4}
10^{-3}
10^{-2}
10^{-1}
10^{0}
10^{1}
Viral replication rate (hour^{-1})

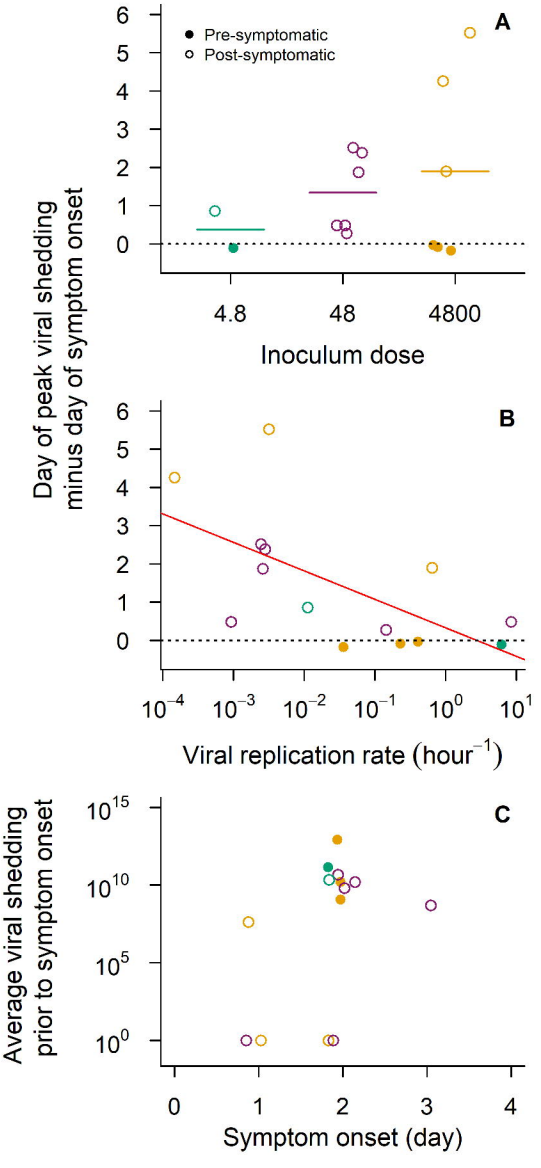
A
Pre-symptomatic
Post-symptomatic
Day of peak viral shedding minus day of symptom onset
6
5
4
3
2
1
0
4.8
48
4800
Inoculum dose
B
Day of peak viral shedding minus day of symptom onset
6
5
4
3
2
1
0
10^{-4}
10^{-3}
10^{-2}
10^{-1}
10^{0}
10^{1}
Viral replication rate ($hour^{-1}$)
C
Average viral shedding prior to symptom onset
10^{15}
10^{10}
10^{5}
10^{0}
0
1
2
3
4
Symptom onset (day)

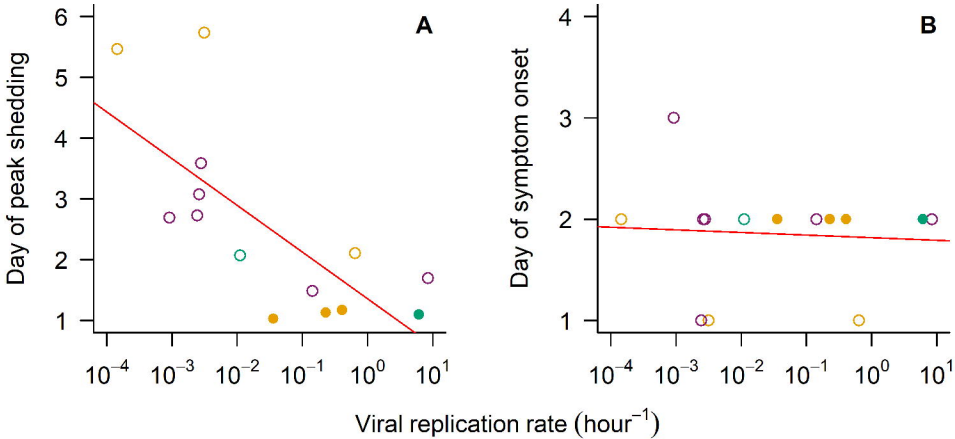
A
B
Day of peak shedding
Day of symptom onset
Viral replication rate (hour^{-1})
1
2
3
4
5
6
10^{-4}
10^{-3}
10^{-2}
10^{-1}
10^{0}
10^{1}

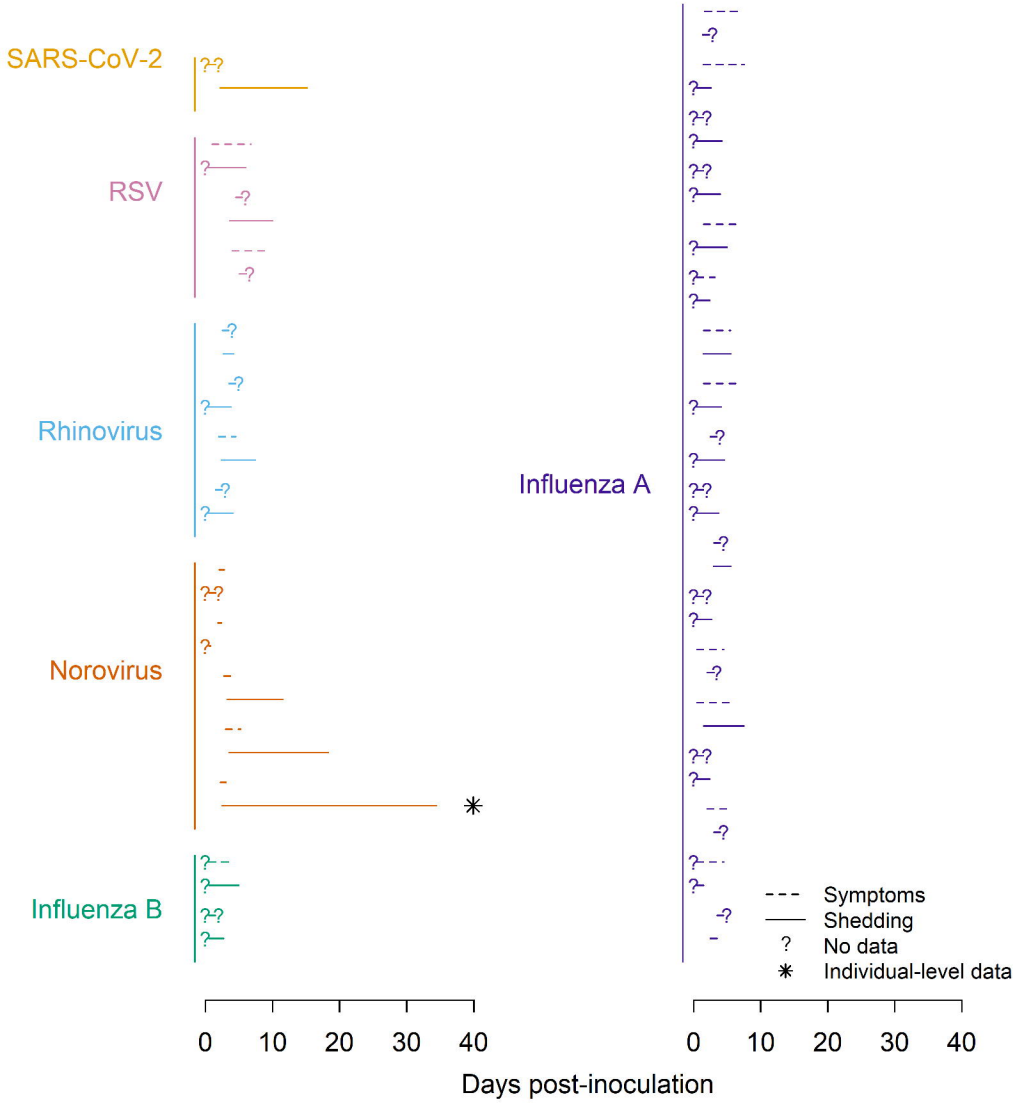
SARS-CoV-2
RSV
Rhinovirus
Norovirus
Influenza B
Influenza A
Symptoms
Shedding
No data
Individual-level data
0
10
20
30
40
Days post-inoculation

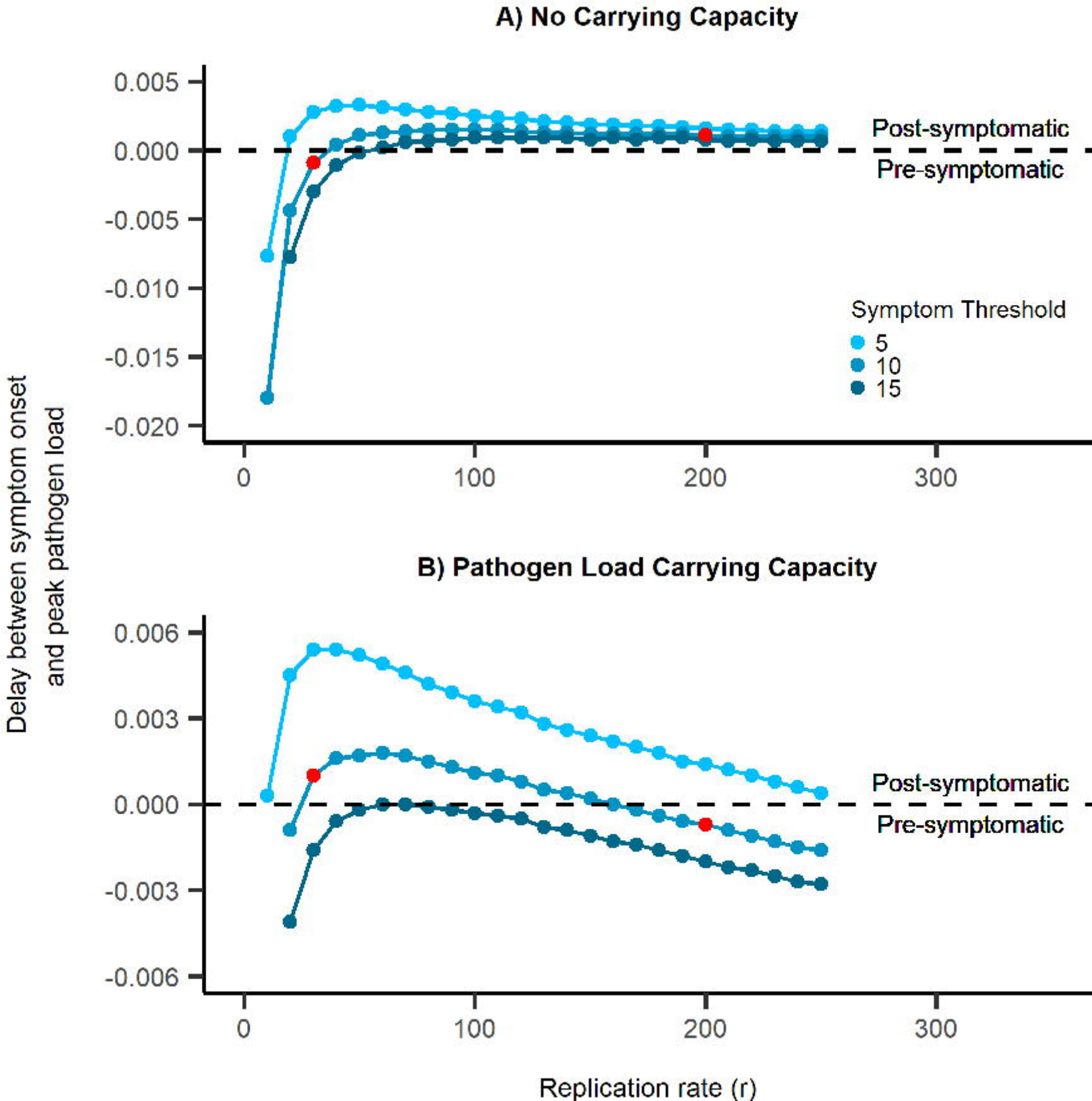
A) No Carrying Capacity
0.005
0.000
-0.005
-0.010
-0.015
-0.020
Post-symptomatic
Pre-symptomatic
Symptom Threshold
5
10
15
0
100
200
300
B) Pathogen Load Carrying Capacity
0.006
0.003
0.000
-0.003
-0.006
Post-symptomatic
Pre-symptomatic
0
100
200
300
Delay between symptom onset and peak pathogen load
Replication rate (r)

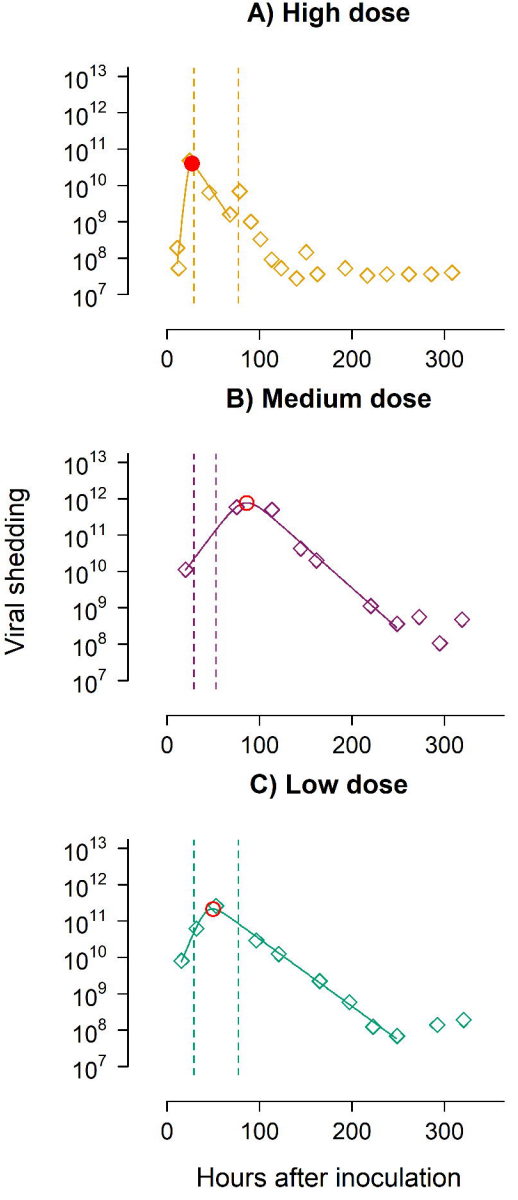
A) High dose
B) Medium dose
C) Low dose
Viral shedding
Hours after inoculation
10^{13}
10^{12}
10^{11}
10^{10}
10^{9}
10^{8}
10^{7}
0
100
200
300

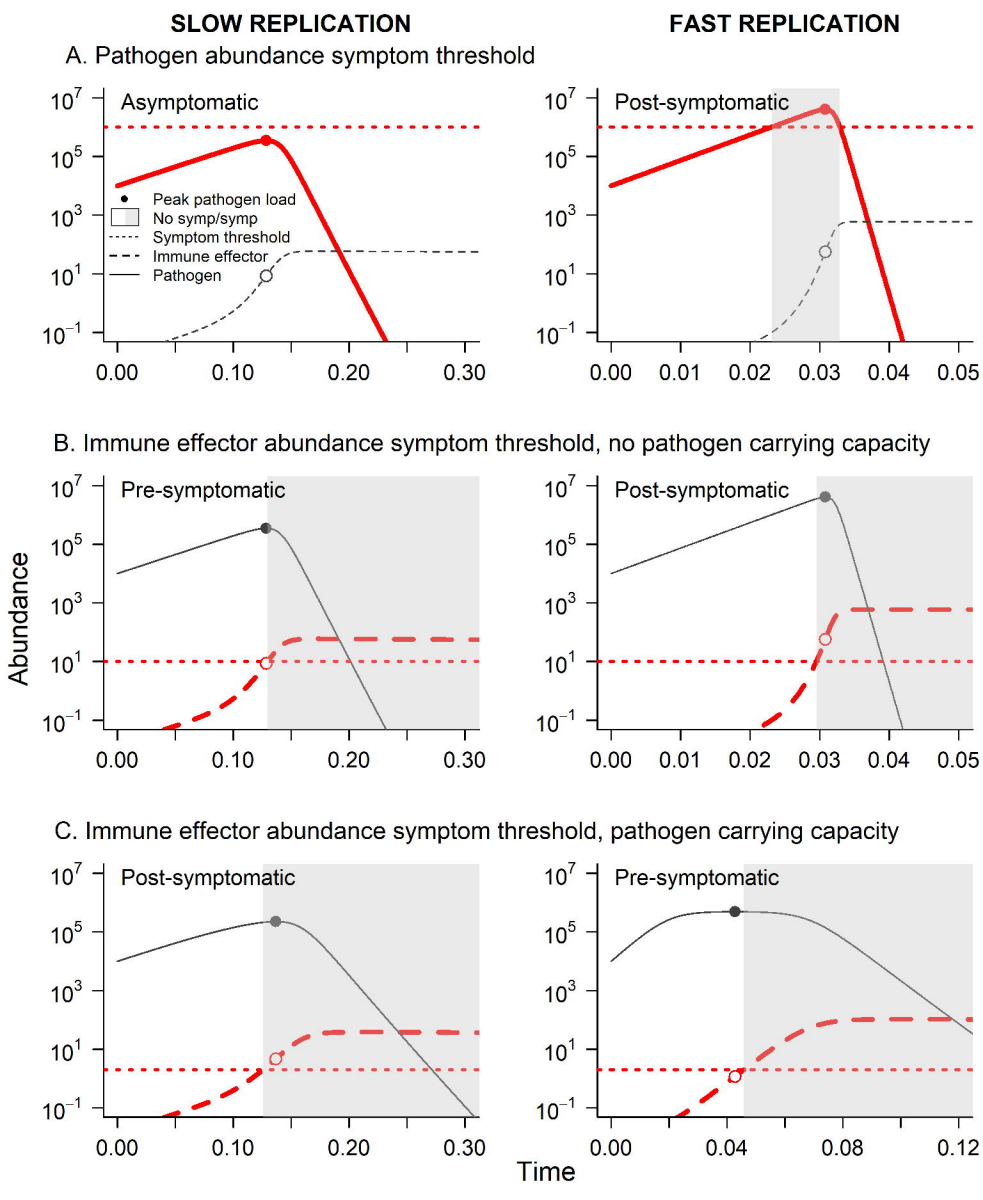
SLOW REPLICATION
FAST REPLICATION
A. Pathogen abundance symptom threshold
Asymptomatic
Post-symptomatic
Peak pathogen load
No symp/symp
Symptom threshold
Immune effector
Pathogen
B. Immune effector abundance symptom threshold, no pathogen carrying capacity
Pre-symptomatic
Post-symptomatic
C. Immune effector abundance symptom threshold, pathogen carrying capacity
Post-symptomatic
Pre-symptomatic
Abundance
Time

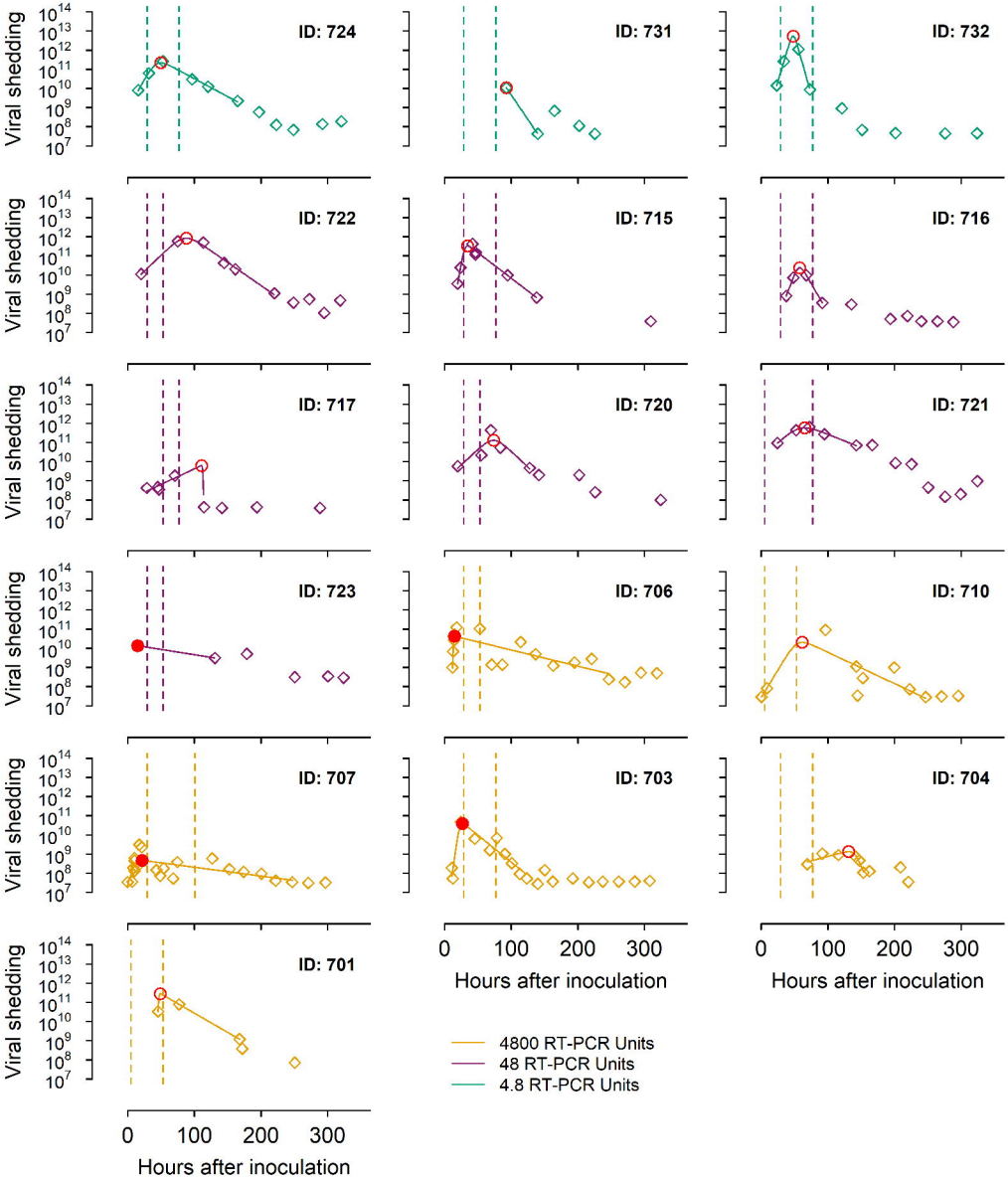
ID: 724
ID: 731
ID: 732
ID: 722
ID: 715
ID: 716
ID: 717
ID: 720
ID: 721
ID: 723
ID: 706
ID: 710
ID: 707
ID: 703
ID: 704
ID: 701
Viral shedding
10^{14}
10^{13}
10^{12}
10^{11}
10^{10}
10^{9}
10^{8}
10^{7}
0
100
200
300
Hours after inoculation
4800 RT-PCR Units
48 RT-PCR Units
4.8 RT-PCR Units

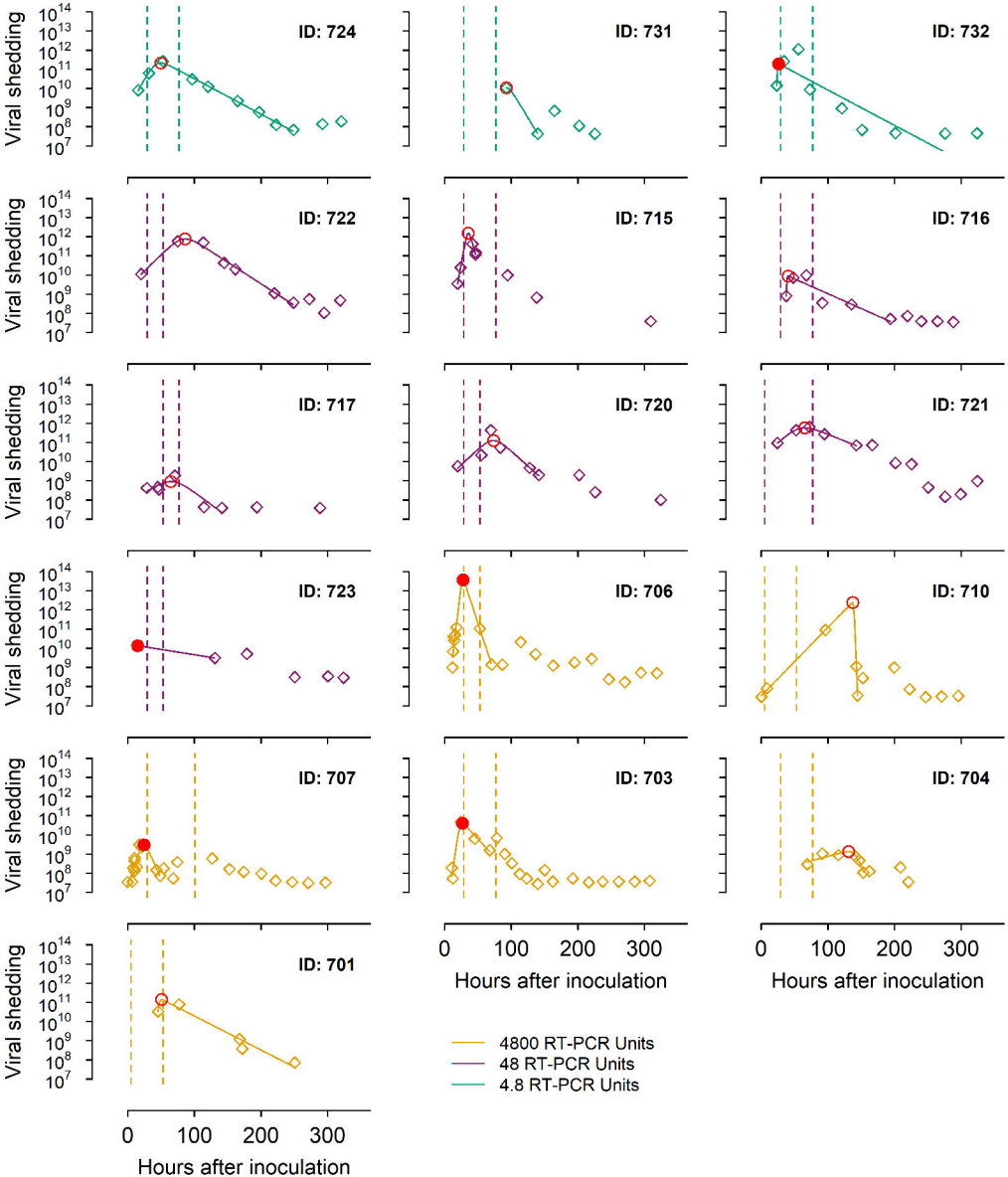
ID: 724
ID: 731
ID: 732
ID: 722
ID: 715
ID: 716
ID: 717
ID: 720
ID: 721
ID: 723
ID: 706
ID: 710
ID: 707
ID: 703
ID: 704
ID: 701
Viral shedding
10^{14}
10^{13}
10^{12}
10^{11}
10^{10}
10^{9}
10^{8}
10^{7}
0
100
200
300
Hours after inoculation
4800 RT-PCR Units
48 RT-PCR Units
4.8 RT-PCR Units